The Dissertation Committee for Liang Ma Certifies that this is the approved version of the following dissertation:

The Nanomechanics of Polycystin-1: A Kidney Mechanosensor

Committee:

Dr. Andres F. Oberhauser, Ph.D.

Dr. Simon A. Lewis, Ph.D.

Dr. Paul J. Boor, M.D.

Dr. Guillermo A. Altenberg, M.D., Ph.D.

Dr. Roger B. Sutton, Ph.D.

Dean, Graduate School

The Nanomechanics of Polycystin-1: A Kidney Mechanosensor

by

Liang Ma, M.Sc.

Dissertation

Presented to the Faculty
Of
Graduate School of Biomedical Sciences
The University of Texas Medical Branch at Galveston

in Partial Fulfillment
of the Requirements
for the Degree of

DOCTOR OF PHILOSOPHY

Approved by the Supervisory Committee

Dr. Andres F. Oberhauser, Ph.D.
Dr. Simon A. Lewis, Ph.D.
Dr. Paul J. Boor, M.D.
Dr. Guillermo A. Altenberg, M.D., Ph.D.
Dr. Roger B. Sutton, Ph.D.

Key words: Polycystin-1, mechanical stability, pathogenic mutations, AFM, Osmolytes,

The University of Texas Medical Branch

August, 2010
Galveston, Texas

Dedication

To my family

Acknowledgements

First and foremost, I would like to thank my mentor, Dr. Andres Oberhauser who provided wonderful training and who was a constant source of instruction and inspiration. I deeply acknowledge him for his encouragement, support and guidance throughout my graduate study. Everything presented in this dissertation would not have been possible without him.

I want to give many thanks to my committee members, Dr. Simon Lewis, Dr. Paul Boor, Dr. Guillermo Altenberg and Dr. Roger Bryan Sutton, for their guidance and involvement throughout the course of this research.

I am grateful to my excellent colleague, Dr. Tzuni Garcia, who was always ready to help, and showed me the greatest "troubleshooting" skill for AFM. I also appreciate the great help and instruction from Dr. Meixiang Xu, who is an expert in molecular biology and showed me the expertise of protein expression and purification.

I especially thank Dr. Henry F. Epstein, our esteemed Chair of department of NCB, who has been always encouraging and helping students to resolve any problem we faced. He led and organized a wonderful local seminar series to encourage every scientific researcher to be involved in studying and discussing the advanced scientific topics and sharing our research processes. I am very grateful to him for his advice and help.

Many thanks to Dr. Wayne Bolen for taking personal attention to my omsolyte experiments. The discussions which I had with him have enriched me and provided me many ideas in finishing this project.

I also want to express my gratitude to Dr. Cary Cooper, Dr. Dorian Coppenhaver, Mrs. Laura Teed and the staff in Graduate School of Biomedical Sciences for their administrative support and help in my graduation.

I recognize the staff of Department of Neuroscience and Cell Biology at UTMB, especially Lisa Davis and Julie Melchor, who helped me a lot in the arrangement of my defense.

I express my greatest gratitude to all the brothers and sisters in my church who were praying for my successful graduation.

My special thanks to all my friends at UTMB for their help and support in the past four years.

Finally, my deeply thanks go to my family for their consistent support and encouragement. I want to thank my wife who is always beside me and also my endless source of motivation. The last but the most, great love and thanks to my eight months old daughter, Joanna, who is all my strength to finish my degree.

The Nanomechanics of Polycystin-1: A Kidney Mechanosensor

Publication No._____

Liang Ma, M.Sc.

The University of Texas Medical Branch at Galveston, 2010

Supervisor: Andres Oberhauser

Mutations in polycystin-1 (PC1) can cause Autosomal Dominant Polycystic Kidney Disease (ADPKD), which is a leading cause of renal failure. The available evidence suggests that PC1 acts as a mechanosensor, receiving signals from the primary cilia, neighboring cells, and extracellular matrix. PC1 is a large membrane protein that has a long N-terminal extracellular region (about 3000 aa) with a multimodular structure including sixteen Ig-like PKD domains, which are targeted by many naturally occurring missense mutations. Nothing is known about the effects of these mutations on the biophysical properties of PKD domains. In addition, PC1 is expressed along the renal tubule, where it is exposed to a wide range of concentration of urea. Urea is known to destabilize proteins. Other osmolytes found in the kidney such as sorbitol, betaine and TMAO are known to counteract urea's negative effects on proteins. Nothing is known about how the mechanical properties of PC1 are affected by these osmolytes. Here I use nano-mechanical techniques to study the effects of missense mutations and effects of denaturants and various osmolytes on the mechanical properties of PKD domains. Several missense mutations were found to alter the mechanical stability of PKD domains resulting in distinct mechanical phenotypes. Based on these findings, I hypothesize that

missense mutations may cause ADPKD by altering the stability of the PC1 ectodomain, thereby perturbing its ability to sense mechanical signals. I also found that urea has a significant impact on both the mechanical stability and refolding rate of PKD domains. It not only lowers their mechanical stability, but also slows down their refolding rate. Moreover, several osmolytes were found to effectively counteract the effects of urea. Our data provide the evidence that naturally occurring osmolytes can help to maintain Polycystin-1 mechanical stability and folding kinetics. This study has the potential to provide new therapeutic approaches (e.g. through the use of osmolytes or chemical chaperones) for rescuing destabilized and misfolded PKD domains.

Table of Contents

List of Tables

List of Figures

Chapter 1

General Introduction

1.1 Autosomal Dominant Polycystic Kidney Disease (ADPKD)

ADPKD is one of the most common life-threatening genetic diseases affecting ~600,000 Americans and 12.5 million people, worldwide. Usually, around one million nephrons are in the cortex of each kidney, and each one contains the glomerulus-tubule structure which carries out the function of purification and filtration of the blood. In ADPKD patients, abnormal fluid-filled cysts develop progressively from renal tubules, resulting in the massive enlargement of the kidneys and ultimately renal failure in more than 50% of the affected individuals (Gabow 1990; Pirson *et al.* 1998). This disease may also damage the liver, pancreas and rarely in heart and brain. ADPKD affects 1 in 400 to 500 newborns, children and adults regardless of sex, age, race or ethnic origin. Parents with ADPKD have a 50 percent chance of passing the disease on to each of their children. It is phenotypically and genetically heterogeneous that 85% of the cases are caused by mutations in the PKD1 gene (the international polycystic kidney disease consortium, 1995), while the remainder result from PKD2 mutations (Mochizuki, *et al.* 1996). The two proteins polycystin 1 and polycystin 2 (PC1 and PC2), encoded by PKD1 and PKD2 genes respectively, may function together as a heterodimeric complex through the C-terminal coil-coiled connection (Boletta *et al.* 2003; Sutters 2006) (**Figure 1**). The available evidence shows that the polycystin complex PC1-PC2 is a shear-stress-activated Ca^{2+} channel involved in regulating many biological processes, such as cation transport, proliferation, apoptosis, cell adhesion and tubulogenesis. In ADPKD patients, the sensing mechanism for tubule size seems lost; thereby cysts develop and enlarge progressively, in a process that ultimately causes renal failure. However, the function of PC1 as well as the

mechanisms whereby mutations in this protein lead to changes in signaling pathways that control cell proliferation, apoptosis, cell adhesion and tubulogenesis remain unknown.

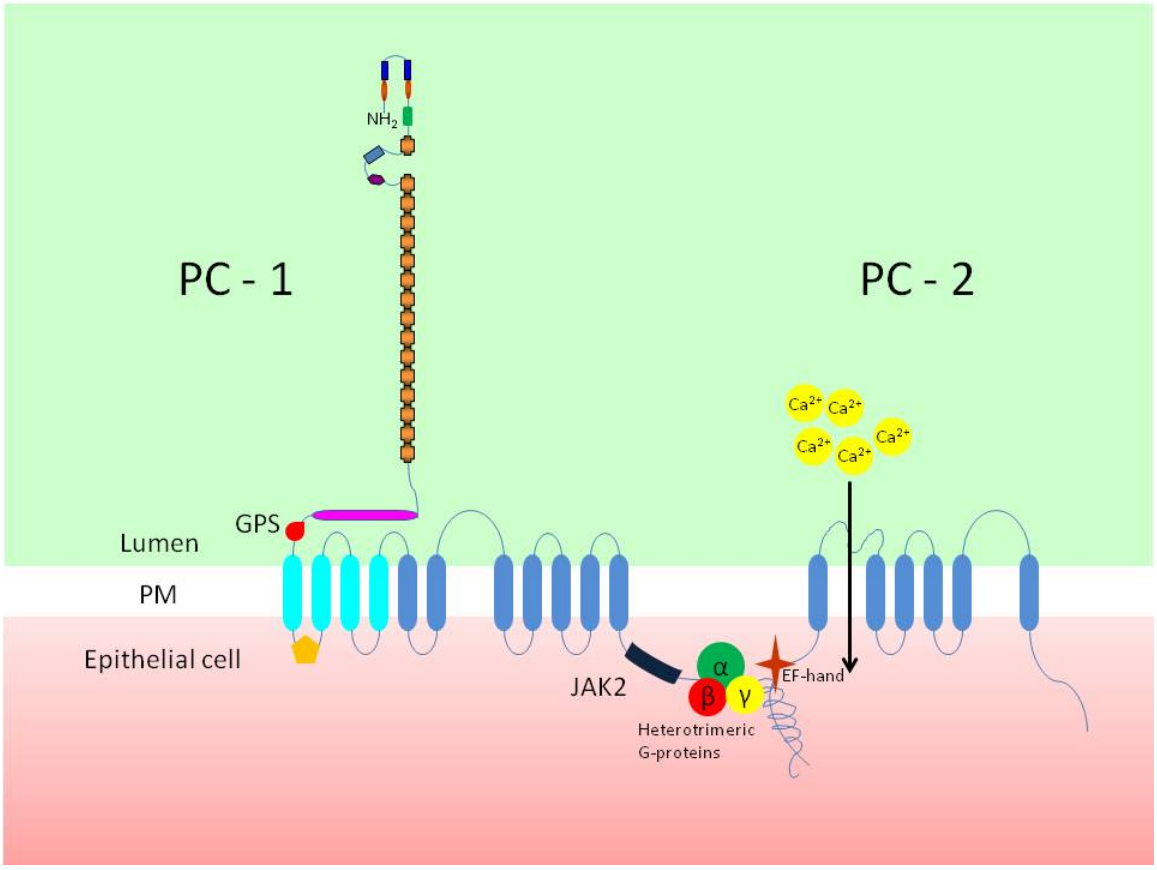

Figure 1: PC-1 and PC-2 are both transmembrane proteins that interact to form a functional complex

1.2 PC1 AND ITS FUNCTION

Immunolocalization studies in normal and ADPKD tissues have shown that PC1 is a cell surface protein in kidney epithelia cells and it localizes to the cell-cell contacts such as adhesions junctions and focal densities at the basal membrane in contact with the extracellular matrix (ECM) and also in the central apical cilia of kidney epithelial cells (Nauli *et al.* 2003). They locate on proximal ducts at young age and mostly locate on

distal and collecting duct at adult age (Geng *et al.* 1996; Palsson *et al.* 1996; Geng *et al.* 1997; Ibraghimov-Beskrovnaya *et al.* 1997). PC1 is a 4302 amino acid (aa) protein with a large multi-modular N-terminal extracellular region of ~3100 aa, 11 transmembrane domains and a shorter 200 aa intracellular C-terminal domain (Hughes *et al.* 1995). The N-terminal ectodomain contains a novel combination of modular domains (**Figure 1**): two leucine-rich repeats (LRR) with flanking cysteine-rich sequences (CRS) (a total of 250 aa long), a C-type lectin Domain (130 aa long), a low-density-lipoprotein-like domain (LDL-A domain), 16 (15 in tandem) Ig-like domains (PKD domains, 90 aa each) and a ~1000 aa segment that is homologous to receptor for egg jelly (REJ) in sea urchin (Moy *et al.* 1996; Sandford *et al.* 1997). PC2 is a 968 aa six transmembrane-spanning protein, with homology to voltage-gated Ca^{2+} and Na^{+} channels, and transient receptor potential (TRP) channels (Ikeda *et al.* 2002). It has been reported that the heterodimerization between PC1 and PC2 is required in order to produce the cation-permeable channel activity (Qian *et al.* 1997; Hanaoka *et al.* 2000; Tsiokas *et al.* 2007).

Based on its structure, PC1 has been suggested to function in three locations of epithelial cells, acting as a cell adhesion protein with mechano-sensing properties (**Figure 2**). These include: 1) in the primary cilium where it senses and transduces mechanical forces (shear flow) into intracellular signals (such as calcium influx and transcription factors), 2) in cell-matrix interfaces where interacts with components of the ECM, and 3) at cell-cell junctions where interacts with neighboring PC1 from adjacent cells.

The group of Zhou (Harvard Medical School) carried out experiments to test primary cilia's function (Nauli *et al.* 2003). The Ca^{2+} influx, which happens in response to mechanical flow stimulation, requires fully developed cilia. The authors found that partially differentiated and non-differentiated cells, where cilia were absent, did not respond to mechanical flow stimuli. In addition, primary cilia were found to mediate the

mechanical flow–induced extracellular Ca^{2+} influx (Praetorius *et al.* 2001; Nauli *et al.* 2003; Praetorius *et al.* 2003). These experiments support the idea that the primary cilium works as mechanosensor in kidney cells.

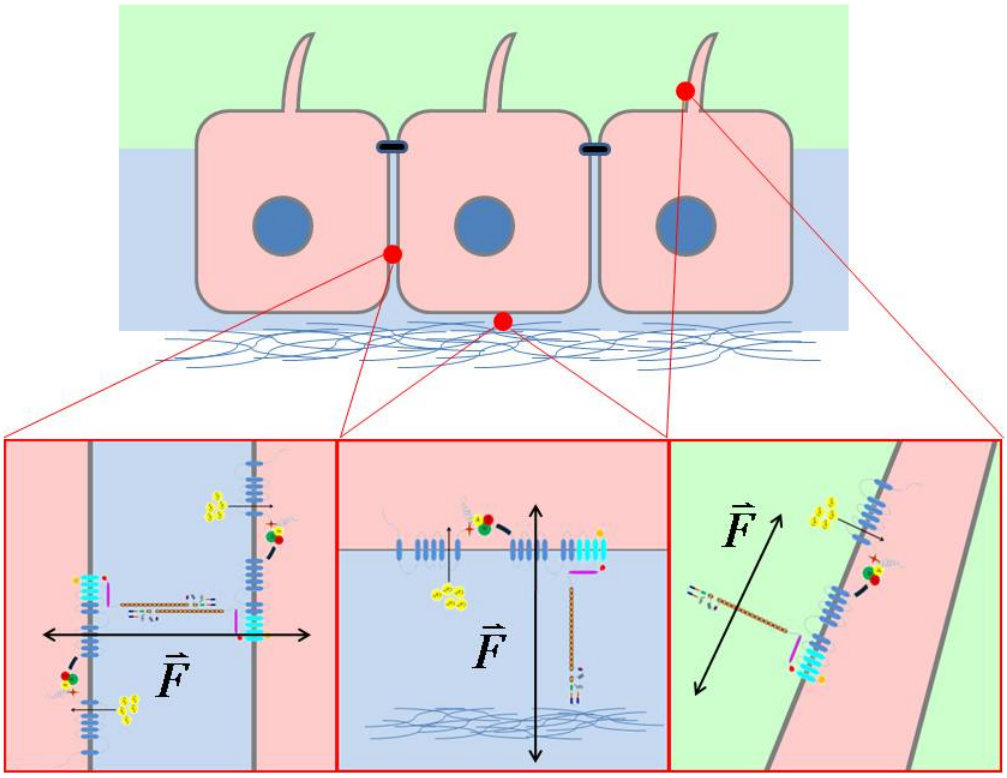

Figure 2: **Subcellular locations of Polycystin-1.** PC1 exists in close association with PC2 at points of points of cell-matrix contact, cell-cell contacts and in the primary cilia of kidney cells. All these locations are subjected to mechanical forces $\vec{F}$ (presented by arrows).

Immunolocalization studies revealed that PC1 and PC2 are localized in the cilia of kidney epithelia cells. Kidney tubular epithelial cells isolated from knock-out mice that lack the PC1 ectodomain, do not respond to mechanical flow. In addition, specific antibodies against PC1 ectodomain were found to block the PC2 (Ca^{2+} channel)'s

opening activity and Ca-influx (Nauli *et al.* 2003). The current hypothesis is that shear stress bends the cilia and so activates PC1, which transduces the mechanical signals through PC2 into chemical signals (Ca^{2+} influx), and other signals that control cell growth and tissue development. These events are important in the maintenance of the shape and dimensions of the renal tubule epithelium (**Figure 3**).

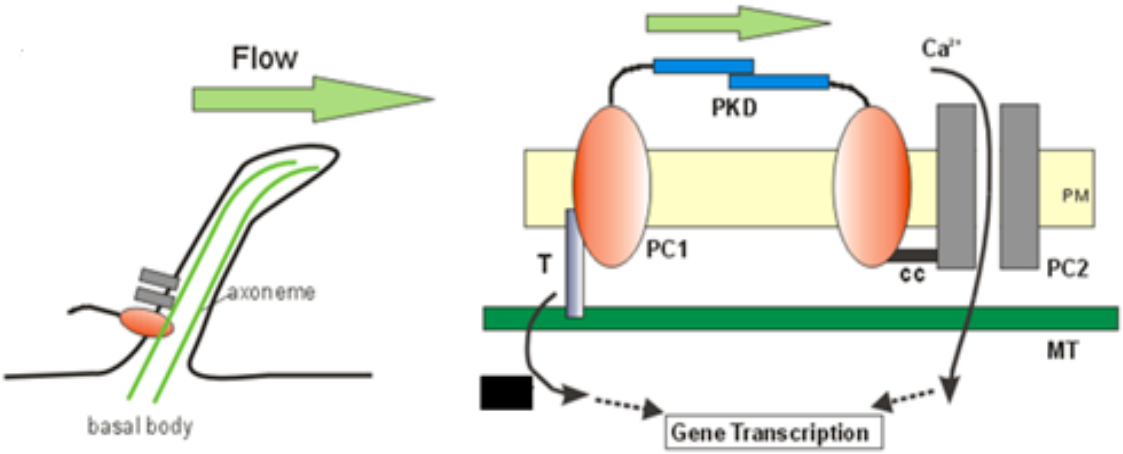

Figure 3: **Model for polycystin complexes and mechanical-transduction in renal epithelia.** Diagram shows that the PC1-PC2 complex in the primary cilium. The mechanical shear forces stretch PC1's ectodomain triggering the opening of the PC2 channel by a direct coupling via the C-terminus coil-coiled (CC) regions. In this model, PC1 is firmly anchored to the microtubules (presented as MT) via tethering molecules (presented as T).

1.3 MISSENSE MUTATIONS

1.3.1 Mutations in PC1.

To date, about 860 mutations have been identified in the PKD1 gene. Among them, about 100 mutations are considered highly likely pathogenic, 30 are considered to be likely pathogenic, 357 of them are thought to be likely polymorphisms and 67 mutations are indeterminate (Autosomal Dominant Polycystic Kidney Disease (ADPKD) Database (PKDB), *http://pkdb.mayo.edu/*). Many are either point mutations or

deletions/insertions mutations that introduce frame shifts and stop codons leading to premature termination. The most likely effect of these types of mutations is a complete loss of normal PC1 function. However, there are also ~260 missense mutations that result in non-conservative amino acid substitutions involving residues that form part of the LRR, PKD repeats or the REJ domain. Missense mutations are point mutations where one nucleotide is changed generating a different codon for a different amino acid. In ADPKD, many missense mutations are found in conserved residues where they are critical to maintain protein's secondary structure or function (to be discussed in Chapter 3). Hence, this kind of substitution might render the mutated protein nonfunctional, and leading to a pathogenic form. According to the ADPKD database, 93 missense mutations are found in PKD domains and 81 missense mutations target the REJ region. However, not all missense mutations are considered to be disease causing. Some are neutral polymorphic mutations when an amino acid is replaced by one of very similar chemical properties or the replacement occurs in a non-conservative region of the protein.

1.3.2 Effects of missense mutations on the mechanical and functional properties of PC1.

Mutations may cause changes in conformation, disrupt the structure of the domains (and cause unfolding or misfolding), or affect their surface properties, as has been suggested for other Ig-like proteins (Bateman *et al.* 1996; Randles *et al.* 2006). PC1'e ectodomain is mainly composed of rigid Ig-like domains, such as PKD domains. Thus, mutations in the ectodomain may cause conformational changes resulting from the disrupted domains, therefore impacting PC1's normal mechanosensing function.

1.4 OSMOLYTES

PC1 is found expressed in different segments of the nephron depending on different age, such as in the proximal tubule at the young age, in distal tubule and collecting duct at adult age. The urea concentration in mammalian kidneys can vary between ~5mM to ~1000 mM from proximal tubule to collecting duct (Goyton 1997; Bedford *et al.* 2007). Also in response to pathological conditions the level of urea is altered (Goyton 1997). Urea is a common chemical denaturant of proteins. PC1 was recently identified as a mechanosensor that senses mechanical cues such as shear flow in the kidney tubule and converts them into various signaling events (Nauli *et al.* 2003; Nauli *et al.* 2004). Hence it is possible that PC1 domains, such as PKD and REJ, may unfold and refold in vivo in response to both mechanical and chemical forces. Its unique function makes it an exciting model to understand how a protein maintains its mechanical function under the harsh conditions found in the kidney.

The native conformation of proteins can be stabilized by naturally occurring osmolytes (such as TMAO, betaine, sucrose, trehalose, sarcosine, sorbitol, glycerophosphorylcholine (GPC), proline and glycerol (Street *et al.* 2006). These 'protecting' osmolytes are small organic molecules which are found in the kidneys from elasmobranches to humans (Yancey *et al.* 1982; Garcia-Perez *et al.* 1991; Schmolke *et al.* 1996b; Venkatesu *et al.* 2009). It was found that the distribution of osmolytes in mammalian kidneys shows an increasing pattern along their corticomedullary axes. Sorbitol, GPC and betaine usually reach to a maximum level at the tip of the papilla where collecting ducts are found (Garcia-Perez *et al.* 1991).

The mechanisms by which osmolytes promote protein folding, increase protein stability and induce conformational changes has been the focus of intense investigation (Baskakov *et al.* 1998; Kumar *et al.* 1999; Bolen 2001; Ratnaparkhi *et al.* 2001; Zou *et*

al. 2002; Auton *et al.* 2005; Ignatova *et al.* 2006; Street *et al.* 2006; Beck *et al.* 2007; Loo *et al.* 2007; Street *et al.* 2009; Venkatesu *et al.* 2009).

1.5 ATOMIC FORCE MICROSCOPY (AFM)

To understand how PC1 senses and mediates mechanical forces requires detailed knowledge of its mechanical properties at the molecular level. One technique that has been widely employed to investigate the mechanical properties of single proteins is atomic force microscopy (AFM) (Oberhauser *et al.* 2008). AFM in its single-molecule force spectroscopy mode is one of the most common nanomanipulation techniques used for the study of the mechanical properties of proteins. For AFM studies, a cantilever is used to pick up and stretch a pre-immobilized protein molecule on a substrate, either from its N-terminal or C-terminal end (**Figure 4A**). To facilitate the AFM experiments, especially the refolding experiments, one of the best strategies is to construct a polyprotein with tandem repeats of desired domains (**Figure 4B**).

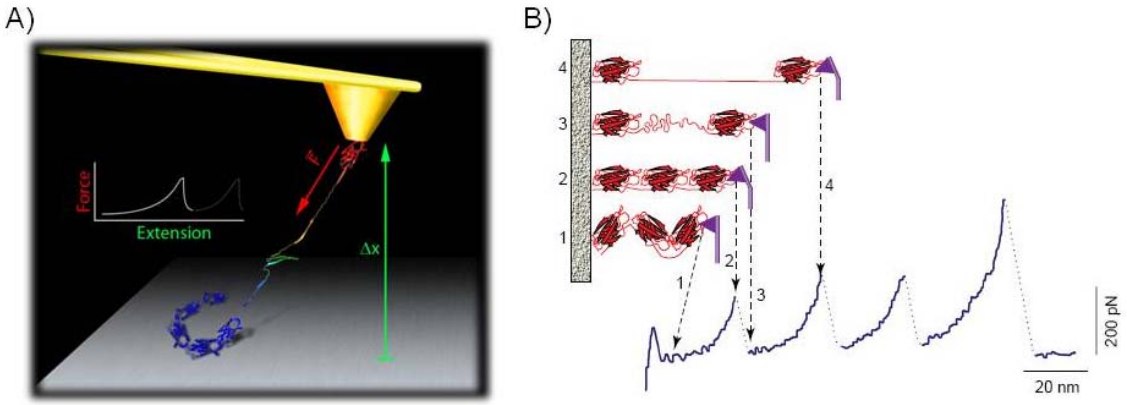

Figure 4: **AFM and Sawtooth pattern.** A) It shows a cantilever picks up a protein molecule and stretches it. The force used to unfold a protein domain will be recorded by the movement of cantilever (Hook's Law). B) Stretching a protein molecule with three tandem repeat domains results in a sawtooth pattern presenting the sequential unfolding of the domains.

Stretching such a polyprotein, a typical saw-tooth pattern can be obtained resulting from the sequential and abrupt unfolding of each individual domain. From the data, not only the elastic properties (in extension, Δx) of the protein, but also mechanical stability (in force, pN) and unfolding kinetics could be investigated.

1.6 AIMS AND OBJECTIVES

PC1 is suggested to be involved regulating many biological processes associated with mechanical forces in the kidney and in other tissues and organs. For example, PC1 plays a role in regulating pressure-sensing in arterial myocytes (Sharif-Naeini *et al.* 2009). Based on the structural similarities between PC1 ectodomain and other modular proteins that have elastic properties it has been hypothesized that PC1 functions mechanically in the primary cilium, cell-cell junctions and the cell-matrix where is subjected to mechanical forces (Qian *et al.* 2005). ***My hypothesis is that PC1 ectodomain possesses novel mechanical properties, making it an ideal mechanosensor in the kidney tubule.*** I propose that the sheer force in tubule directly act on PC1 via stretching its ectodomain and activate the associated polycystin-2 (PC2) Ca^{2+} ion channel.

Very little is known about how mutations might alter PC1's structure and mechanical properties. Also, it is not known how its mechanical properties are affected by the chemical microenvironment in the renal tubule, for example, a wide range of concentrations of urea and pH (ca.4-8) levels. Urea and pH may modify the mechanical properties of normal PC1 which may lead to changes in the mechanical function mediated by PC1 along the renal tubule. I propose that naturally occurring osmolytes can counteract the destabilizing effects of urea on PC1 *in vivo*.

The main goal of the project discussed in the present dissertation is to quantitatively examine the mechanical and biophysical properties of the extracellular

region of wild type and mutant forms of PC1 in different environments that mimic *in vivo* conditions.

The Specific Aims are:

1) To determine the effects of naturally occurring missense mutations on the stability of individual PKD domains. The results are described in Chapter 3.

2) To test the hypothesis that naturally occurring osmolytes in kidney affect the mechanical properties of individual PKD domains. The results are described in Chapter 4.

1.7 SIGNIFICANCE OF THIS PROJECT

My long term goals are to elucidate the structure and biophysical properties of the PC1, to understand i) the effects of missense mutations and ii) the interplay between denaturant and protecting osmolytes on PC1's mechanical function. This study should thus provide a solid basis to investigate the molecular mechanisms of the signaling events that link PC1 mutations with the ADPKD phenotype. Furthermore, these studies have the potential to provide new therapeutic approaches (e.g. through the use of osmolytes) for rescuing destabilized PKD domains.

Chapter 2

Materials and Methods

2.1 Introduction

AFM has been widely employed to investigate the mechanical properties of single proteins (Fisher *et al.* 1999a; Fisher, *et al.* 1999b; Mehta *et al.* 1999; Carrion-Vazquez *et al.* 2000; Fisher *et al.* 2000; Samori 2000; Best *et al.* 2002a; Rief *et al.* 2002; Rounsevell *et al.* 2005; Linke *et al.* 2008; Oberhauser *et al.* 2008; Muller *et al.* 2009). AFM in its single-molecule force spectroscopy mode is one of the nanomanipulation techniques used for the study of the mechanical properties of proteins (**Figure 5**).

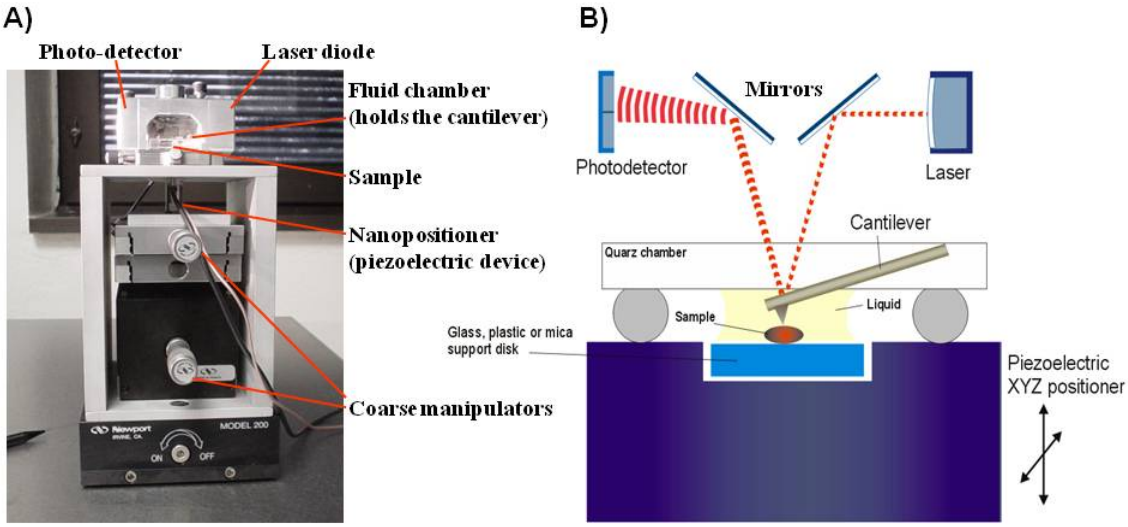

Figure 5: **AFM setup and its components. A)** A picture of our home-built AFM. It contains two main components: a piezoelectric positioner (in bottom metal frame) and an optical head (top silver metal box). The nanopositioner is a piezoelectric device, which is allowed to move in the X, Y, Z dimensions. **B)** Schematic diagram of our AFM. A laser diode in the optical head emits a red beam laser that is reflected from the back of the cantilever into a split photodiode detector, where the output is calibrated in Force units (Newtons). The quartz chamber is used to hold the cantilever and immerse the sample in saline. The sample is moved by controlling the piezoelectric positioner.

2.2 MATERIALS AND METHODS

2.2.1 Surfaces for AFM experiments

Usually, different kinds of surfaces, such as glass, Ni-NTA, Silanized glass and gold coated glass, have been used to adsorb different polymers and proteins in AFM experiments. Here, several methods are described for preparing the functionalizing glass coverslips.

2.2.1.1. Glass coverslips

Reagents:

1. MilliQ H_2O (18.2 MΩ)
2. 70% (v/v) Ethanol
3. 10% (v/v) Hellmanex (for cleaning glass)
4. Parafilm
5. Transferring pipettes

Equipment:

1. Glass Substrates (Round Glass Coverslips, 15 mm diameter, 1oz, Ted Pella, Inc.)
2. 50 ml glass beakers
3. Sonicator
4. Compressed N_2 gas

2.2.1.2. Silanized coverslips

Reagents:

1. MilliQ H_2O (18.2 MΩ)
2. 0.1 M H_2SO_4
3. Trimethylchlorosilane (TMS-Cl)
4. Dry Methanol, acetone, chloroform

Equipment:

1. Glass Substrates (Round Glass Coverslips, 15 mm diameter, 1oz, Ted Pella, Inc.)
2. 50 ml glass beakers
3. Nitrogen gas (filtered, compressed)

2.2.1.3. Ni-NTA Coverslips

To allow tight binding of the proteins to Ni-NTA, a polyhistidine tag is typically added to the N-terminus of the protein. The glass coverslips (Glass Coverslips, 15mm diameter, 1oz, Ted Pella, Inc.) must be silanized with a derivative of NTA that coordinates nickel. The detailed protocol is described in section 2.2.5.

Reagents:

1. Distilled H_2O
2. MilliQ H_2O (18 MΩ)
3. ~20 ml 20 N KOH
4. Acetic acid
5. 3-mercaptopropyltrimethoxysilane (TSL8380, Toshiba GE Silicone, Tokyo)
6. 50 ml 10 mM MOPS-KOH, pH 7
7. N-[5-(3'-maleimidopropylamido)-1-carboxypentyl] iminodiacetic acid (maleimide-C3-NTA (Dojindo); 20 mg/ml in 10 mM MOPS-KOH
8. 10 ml 100 mM DTT in MilliQ H2O
9. 50 ml 10 mM $NiCl_2$ in MilliQ H2O
10. Parafilm

Equipment:

1. Rocker
2. 50 ml centrifuge tube
3. 50 ml Beakers
4. 2 L Beaker

5. Sand bath
6. Thermometers (110 °C range)
7. Pipette and pipette tips (1 ml)

2.2.2 AFM cantilevers

Two key parameters are used to characterize AFM cantilevers in force spectroscopy measurements: the spring constant, k_C (pN/nm); and the resonant frequency, f_0 (Hz). The spring constant of a typical cantilever, k_C, is in the range of 10–100 pN/nm (for MLCT or MSNL silicon nitride, Veeco). For a cantilever with a k_C of 60 pN/nm, the thermal noise of the force measurements is calculated to be approximately 15 pN rms (the root-mean-square force fluctuation) (Bustamante *et al.* 2000). Most of the AFM cantilevers are available with metal coatings, which are intended to improve the reflectivity of the back side of the cantilevers, such as Aluminum, gold and Platinum. The cantilever that I typically used was silicon nitride gold-coated (MLCT-AUHW, Veeco Metrology Group, Santa Barbara, CA). Another two types of cantilevers MSNL and OBL-105 (Veeco Metrology Group, Santa Barbara, CA) were used for special experiments, such as refolding, etc.

2.2.3 Reagents for expression and purification of PKD polyproteins

1. Vectors: T-A cloning vector pGEM-T vector from Promega; Expression vectors include pEQ80L and pAFM, a modified from pRSET vector (Steward *et al.* 2002).
2. Host cell: *E. coli* Top10 and JM109 are used for plasmid cloning. *E. coli* BL21 and C41 strains are used for protein expression.
3. Media: LB medium (10 g Bacto-Tryptone, 5 g Bacto-yeast extract, 10 g NaCl, in total volume 1 L ddH_2O, adjust pH to 7.0), and YT medium (16 g Bacto-

Tryptone, 10 g Bacto-yeast extract, 5 g NaCl, in total volume 1 L ddH_2O, adjusted to pH 7.2) are used for growing *E. coli*. Before use, antibiotics such as Ampicillin or Kanamicin are supplied into medium at a working concentration of about 100 g/ml.

4. Enzymes: Platinum® Taq DNA Polymerase High Fidelity (Invitrogen) is used in polymerase chain reaction (PCR) to amplify the DNA fragments. Restriction endonucleases such as BamHI/ NheI/ EcoR I/ Not I/ KpnI/ SacI/ XbaI/ SpeI/ NdeI (NEB Inc.) are used for enzyme digestion to obtain DNA fragments and prepare the expression vectors. T4 DNA Ligase from Promega is used in ligation reaction.
5. Kits and others: QIAprep Spin Miniprep Kit is used for plasmid extraction. QIAquick Gel Extraction Kit (Qiagen) is used to purify DNA fragments and vectors from gels after DNA gel electrophoresis. Homemade competent cells are prepared with Z-Competent™ E. Coli transformation Kit (Zymo Research Corp.). Protease Inhibitor Cocktail Tablets, Ni-NTA (nickel-nitrilotriacetic acid) resins, Ni-NTA spin columns and Poly-Prep Chromatography Columns are used during protein purification. PD-10 Columns (GE), Vivaspin series (GE) or Amicon Ultra Centrifugal Filter Devices (Millipore) are used for further protein purification.
6. Protein purification buffers. Cell lysis buffer/column equilibration buffer 1x PBS with 10 mM imidazole, pH 7.4; the wash buffer is 1x PBS with 25 mM imidazole; the elution buffer is 1x PBS with 250 mM imidazole.
7. SDS-PAGE gel analysis: we use phastgel System (GE) for protein analysis.

2.2.4 Cloning, expression and purification of proteins

2.2.4.1 Preparation of PKD DNA fragments

Proper primers were designed to amplify the first PKD domain from human PC1 (HuPKDd1, residues Val-268 – Glu-354) and introduce different pairs of restriction enzyme sequences on both ends by using PCR. Then HuPKDd1 is purified using QIAquick Gel Extraction Kit (QIAGEN) and cloned into pGEM-T vector by ligation reaction. After that, the plasmids were transformed into competent cells and the positive colonies were screened using the blue/white screening method. The plasmids were extracted from the cells with QIAprep Spin Miniprep Kit (QIAGEN). The purified plasmids were digested with restriction enzyme and identified by agarose gel electrophoresis. The positive clones were further confirmed by DNA sequencing.

2.2.4.2 Cloning and expression of a (I27-HuPKDd1)$_3$-I27 hetero-polyprotein

This polyprotein based on HuPKDd1and the titin immunoglobulin domain #27 (I27). The I27 domain has been extensively studied by force spectroscopy hence it can serve as an internal fingerprint (Li *et al.* 2000; Oberhauser *et al.* 2002). We assembled an I27-HuPKDd1 hetero-polyprotein containing three multiples of the I27-HuPKDd1 dimer, by applying a multiple-step cloning technique that makes use of four restriction sequences (BamHI, Bgl II, BstY and Kpn I) (Carrion-Vazquez *et al.* 2000; Qian *et al.* 2005). This construct was cloned in an *E. coli* recombination-defective strain, Sure-2 (Stratagene), and expressed in the BL21 strain.

2.2.4.3 Preparation of expression vectors

Vectors pQE80L, pAFM (modified from pRSET A vector (Steward *et al.* 2002; Rounsevell *et al.* 2005) and p202 (vector with MBP), were used to express PKD polyproteins in *E. coli*. All the vectors were digested with proper pairs of restriction

enzymes in order to match the insert HuPKDd1 fragment. The digested vectors were recovered by QIAquick Gel Extraction Kit (QIAGEN).

2.2.4.4 Ligation and transformation

The insert DNA fragment and vector were mixed in the range of 3:1 (molar ratios) to carry out a regular ligation reaction with a final volume of 10 ul and incubate overnight at 16 °C. The *E. coli* Top10 and JM109 cells were used for cloning and the BL21 and C41 cells are used for protein expression.

2.2.4.5 Expression of the polyproteins

E.coli expression protocol is modified from the manual of pRSET A for high-level expression of recombinant proteins (Invitrogen, Catalog no. V351-20). The cells were incubated with vigorous shaking in LB or YT media supplied with antibiotics at 37 °C. When OD600 reached ~0.6, the protein expression was induced by adding IPTG to a final concentration of 1mM to 5mM**.** The cells were incubated over night at 16 °C with shaking.

2.2.4.6 Purification of the polyproteins

1. Cell lysis: Dissolve the cell pellets in the lysis buffer (with protease inhibitors) in an ice bath. The cells were lysed by sonication or by using a fluidizer or emulsifier. During the procedure, always keep the samples in ice bath. Centrifuge the lysate to collect the supernatant for purification.
2. Purification: Ni-NTA resins were used to purify PKD polyproteins. Before use, the resins were equilibrated with lysis buffer. Then, the supernatant of cell lysate was mixed with the resins and kept rocking for 30–60 minutes at 4 °C in order to achieve the thorough binding between His tagged protein and Ni-NTA resin. The supernatant was collected when being driven though the settled resins by gravity. The wash buffer (containing 40 mM imidazole) was used to wash off the

unwanted proteins through non-specific binding. The proteins were eluted by adding 1 ml elution buffer (containing ~250 mM imidazole) and stored at 4 °C. The proteins were identified and analyzed by running a SDS-PAGE gel with proper size range markers.

3. Desalting and concentrating: PD-10 Columns were used to remove the high concentration salt (e.g. imidazole). Vivaspin series or Amicon Ultra Centrifugal Filter Devices were used to concentrate the proteins.

2.2.4.7 Cloning, expression and purification of an archaea PKD domains (ArPKD)

The ArPKD monomer gene was cloned from a construct kindly supplied by S. Qamar and R. Sandford (University of Cambridge, UK) and ligated into a modified pRSETA vector (Invitrogen). Standard site-directed mutagenesis reactions were used to introduce mutations into individual domains. Two ArPKD polyproteins were prepared to facilitate the AFM experiments. One containing seven repeats of ArPKD domains, polyArPKD was constructed using a multiple-step cloning technique as described in (Steward *et al.* 2002; Forman *et al.* 2009). The other construct was a homopolyprotein containing many (>10) ArPKD domains made using a cysteine-based polymerization strategy, as described in (Dietz *et al.* 2006). This consists of adding cysteines residues to both N- and C- termini by mutagenesis reaction. The proteins were expressed and purified as described previously (Forman *et al.* 2005; Dietz *et al.* 2006). The two-step purification procedure involved nickel affinity chromatography followed by gel filtration.

2.2.5 Preparation of surfaces

2.2.5.1 Glass coverslips

1. Take around 20 coverslips (Round Glass Coverslips, 15mm diameter, 1oz, Ted Pella, Inc.) and put them into a 50 ml beaker.

2. Spray 70% (v/v) EtOH on the coverslips and pipette to get rid of the dust on the surface of the glass coverslips.
3. Rinse with MilliQ H_2O until the solution is clear.
4. Add 30 ml 10% (v/v) Hellmanex (3 ml Hellmanex into 30 ml MilliQ H_2O) and wash the coverlips thoroughly.
5. Cover the beaker with Parafilm and sonicate for 20 mins.
6. Discard the Hellmanex solution and rinse the coverslips with MilliQ H_2O.
7. Rinse the coverslips with 70% (v/v) EtOH.
8. Rinse the coverslips with MilliQ H_2O to remove the alcohol.
9. Add 30 ml MilliQ H_2O and sonicate for 20 mins.
10. Discard the MilliQ H_2O and add 20 ml fresh MilliQ H_2O, covered by parafilm and store at room temperature until further use.
11. Before use, the coverslips should be dried in a stream of N_2 gas.

2.2.5.2 Silanized glass coverlips (Sundberg *et al.* 2003)

1. Dip the glass coverslips in 0.1 M H_2SO_4 for 20 s and rinse with MilliQ H_2O.
2. Dip the glass coverslips for 20 s in each of the following solutions: methanol, dry acetone, and dry chloroform.
3. Dry with nitrogen gas.
4. Dip the glass coverslips in freshly prepared solution of 5% (v/v) trimethylchlorosilane (TMS-Cl) in chloroform for 20 s.
5. Rinse twice in chloroform.
6. Dry with nitrogen gas and store them at room temperature prior to use.

2.2.5.3 Ni-NTA coated glass coverslips (modified from (Sakaki *et al.* 2005))

1. Put ~20 glass coverslips (15 mm diameter, 1oz, Ted Pella, Inc.) into a 50 ml centrifuge tube and immerse them in ~20 ml 20 N KOH, rocking for ~13 h.
2. Rinse with distilled water to completely wash off the KOH by using a 2 L glass beaker.
3. Transfer all the coverslips in to a 50 ml glass beaker and immerse the coverslips in a solution containing 0.02% (v/v) acetic acid and 2% (v/v) 3-mercaptopropyltrimethoxysilane, incubate the beaker on sand bath at 90°C for 1h.
4. Rinse thoroughly with distilled water using the 2 L glass beaker for ~1 hr.
5. Collect all the coverslips and bake them in an oven at 120°C for 10 min.
6. After cooling to room temperature, the SH groups of the saline on the glass surface are reduced by 100 mM DTT for 10 min, then rinse the coverslips with distilled water in a 2 L beaker.
7. React with 20 mg/ml *N*-[5-(3'-maleimidopropylamido)-1-carboxypentyl] iminodiacetic acid (Dojindo) in 10 mM MOPS-KOH for 30 min by pipetting a drop of the solution on the top of each coverslip.
8. Gently rinse the coverslips with MilliQ water.
9. Air-dry the coverslips and add a drop of 10 mM $NiCl_2$ on the top side of coverslip and allow the reaction for 10 min.
10. Repeat step 8 to rinse off the free $NiCl_2$.
11. Air-dry the Ni-NTA coated coverslips and store them in air at room temperature until use.

2.2.6 Calibration of the AFM cantilevers

The spring constant values of AFM cantilevers that originate even from the same batch (wafer) can differ quite significantly (up to ± 30%). Therefore, each individual

cantilever must be calibrated before measurement. In the experiments, I use the so-called thermal method which is based on the energy equipartition theorem (Florin *et al.* 1995). When a cantilever system is modeled as a simple harmonic oscillator, the average potential energy of the cantilever, $1/2k_CZ^2$, is equal to the "thermal energy", $1/2k_BT$, where k_C is the cantilever spring constant, Z is the amplitude of its random oscillations in thermal equilibrium, k_B is the Boltzmann constant, and T is the absolute temperature. Thus, calibrating the cantilever involves the determination of Z^2.

1. Z^2 is not measured directly but is determined from the measurement of V^2, where V is the voltage of the split photodiode generated by the laser beam that traces the movement of the cantilever. To convert V^2 to Z^2, it is necessary to determine the optical lever sensitivity, S, of the photodiode voltage, V, to the amount of the cantilever bending, Z, using the equation $S = V/Z$.
2. To Determine S the cantilever is pushed vertically – and therefore bent – by the piezoelectric actuator of the AFM. Z (in nm) and V (in volts), corresponding to the bending, are directly measured.
3. V^2 is typically not evaluated in the time domain but is converted to the frequency domain by performing the Fourier transform on the time signal, $V_{(t)}$. This approach permits the evaluation and rejection of low-frequency mechanical (non-thermal) noise that contributes to the motion of the cantilever.

2.2.7 AFM experiments

2.2.7.1 Single-molecule atomic force microscopy

The mechanical properties of single proteins were studied using a home-built single molecule AFM as described previously (Oberhauser *et al.* 1998; Carrion-Vazquez *et al.* 1999; Bullard *et al.* 2002; Oberhauser *et al.* 2002; Miller *et al.* 2006). The spring

constant of each individual cantilever was calculated as described in section 2.2.7 using the equipartition theorem (Florin *et al.* 1995). The cantilever spring constant varied between 30 and 50 pN/nm, and root mean square force noise (1-kHz bandwidth) was ~15 pN. Unless noted, the pulling speed of the different force-extension curves was in the range of 0.5 – 0.7 nm/ms.

2.2.7.2 Single protein mechanics

In a typical experiment, a small aliquot of the purified proteins (~1 – 50 µl, 10 – 100 µg/ml) was allowed to adsorb to a suitable substrate (for ~10 min) and then rinsed with phosphate-buffered saline (PBS), pH 7.4. We found that PKD protein constructs adsorbed well to glass, gold-coated glass, or nickel-nitrilotriacetic acid-coated coverslips. Proteins were picked up randomly by adsorption to the cantilever tip, which was pressed down onto the sample for 1 – 2 s at forces of several nanonewtons and then stretched for several hundred nanometers. The probability of picking up a protein was typically kept low (less than 1 in 50 attempts) by controlling the amount of protein used to prepare the coverslips.

2.2.7.3 Analysis of the speed dependence data

The unfolding force distribution and speed dependence of the unfolding forces were fit using Monte Carlo simulation to calculate the unfolding rate constants, α_o, and the position of the transition state, x_u, as described previously (Rief *et al.* 1997; Oberhauser *et al.* 1998; Li *et al.* 2000; Oberhauser *et al.* 2001). The errors in the determination of these parameters were estimated by running the Monte Carlo simulations about 10 times.

Chapter 3: Naturally Occurring Mutations Alter the Stability of Polycystin-1 Polycystic Kidney Disease (PKD) Domains

3.1 INTRODUCTION

Mutations in mechanosensitive proteins typically lead to defects in mechanotransduction and subsequent disturbance of diverse signaling pathways, which has been implicated in developing various diseases from muscular dystrophies to kidney disease (Jaalouk *et al.* 2009). To date, about 860 mutations have been identified in the PKD1 gene (available through the Autosomal Dominant Polycystic Kidney Disease: Mutation Database web site). Most are either point mutations or deletion/insertion mutations that introduce frame shifts and stop codons leading to premature termination. The most likely effect of these types of mutations is a complete loss of normal PC1 function. However, there are also about 260 missense mutations that result in non-conservative amino acid substitutions involving residues that form part of the ectodomain of PC1. Mutations may cause changes in conformation, disrupt the structure of the domains (and cause unfolding or misfolding), or affect their surface properties, as has been suggested for other Ig-like proteins (Bateman *et al.* 1996; Randles *et al.* 2006). However, very little is known about how missense mutations might alter the structure of PC1 and mechanical properties. In this study, we used single-molecule AFM and equilibrium thermodynamics to understand the effect of missense mutations on the mechanical properties of PC1. Six missense mutations (FH26L, T36C, G43S, W38R, R57L, and V59H) were tested on the first PKD domain of PC1, HuPKDd1. We found that these mutations alter the mechanical stability of the domain, resulting in distinct mechanical PKD phenotypes. We find that point mutations can affect the free energy of mechanical unfolding and the position of the transition state. We also found that equivalent mutations in the homologous PKD domain found in *Methanosarcina*

archaebacteria (Jing *et al.* 2002) affect thermodynamic stability. This indicates that pathogenic mutations can affect the normal response of the PKD domain to external mechanical forces and may help understand the molecular mechanisms underlying the physiological effects of mutations in PC1.

3.2 MATERIALS AND METHODS

3.2.1 Cloning and expression of HuPKDd1 constructs for AFM experiments

We cloned and expressed in bacteria a heteropolyprotein based on the first PKD domain from human PC1 (HuPKDd1, residues Val-268 – Glu-354) and the titin immunoglobulin domain 27 (I27). The I27 domain has been extensively studied by force spectroscopy and hence serves as an internal fingerprint (Best *et al.* 2001; Best *et al.* 2002b; Qian *et al.* 2005). We assembled an I27-HuPKDd1 heteropolyprotein using a multiple step cloning technique that makes use of four restriction sequences (BamHI, BglII, BstY, and KpnI) to three multiples of the I27-HuPKDd1 dimer hexamer (Forman *et al.* 2005; Qian *et al.* 2005). The R57L mutant heteropolyprotein was obtained by mutagenesis PCR on the I27-HuPKDd1 construct.

The single-point mutations, T36C, G43S, and V59H, were produced by PCR synthesis using the QuikChange II mutagenesis kit (Stratagene). The cDNAs were subcloned into vector pAFM1 – 8 using the restriction sequences SacI and KpnI (Steward *et al.* 2002). The proteins were expressed and purified as described previously (Forman *et al.* 2005; Qian *et al.* 2005). **Figure 6** shows a typical SDS-PAGE of some of the recombinant HuPKDd1 polyproteins used for AFM. All these proteins expressed well in *E. coli* and were purified from the soluble fraction.

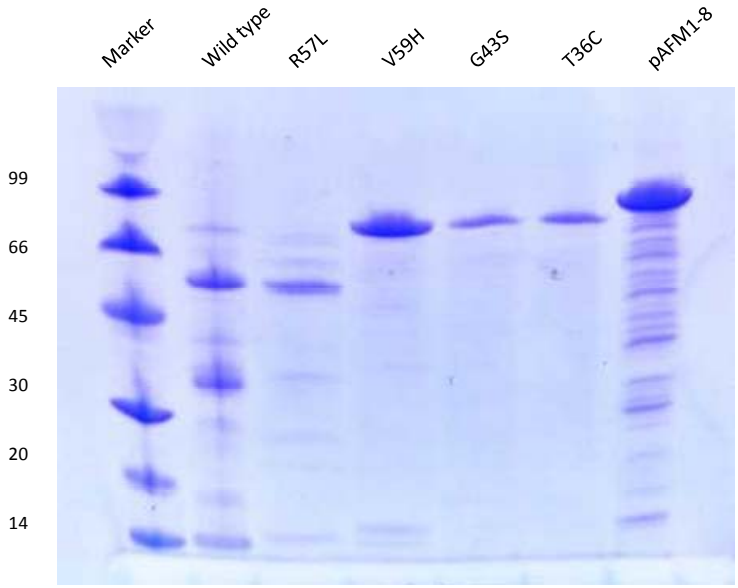

Figure 6: SDS-PAGE (15%) stained with Coomassie brilliant blue of the different HuPKDd1 recombinant proteins used for AFM experiments. Lane 1: low molecular weight-SDS Marker (GE lifescience), lane 2: wild type (I27-HuPKDd1)3 protein, lane 3: (I27-HuPKDd1R57L)3 mutant protein, lane 4: I27- HuPKDd1V59H-(I27)5 mutant protein, lane 5: I27- HuPKDd1G43S-(I27)5 mutant protein, lane 6: I27- HuPKDd1T36C-(I27)5 mutant protein, lane 7: control I27 octamer polyprotein, (I27)8.

3.2.2 Cloning, expression, and purification of archaea PKD domains (ArPKD)

The ArPKD monomer gene was cloned from a construct kindly supplied by S. Qamar and R. Sandford (University of Cambridge, UK) and ligated into a modified pRSETA vector (Invitrogen). Standard site-directed mutagenesis reactions were used to introduce mutations into individual domains. The proteins were expressed and purified as described previously (Forman *et al.* 2005). The two-step purification procedure involved nickel affinity chromatography followed by gel filtration.

3.2.3 Single-molecule atomic force microscopy

The mechanical properties of single proteins were studied using a home-built single molecule AFM as described previously (Oberhauser *et al.* 1998; Carrion-Vazquez *et al.* 1999; Bullard *et al.* 2002; Oberhauser *et al.* 2002; Miller *et al.* 2006).

3.2.4 Equilibrium denaturation of ArPKD domains

All experiments were carried out in phosphate-buffered saline (pH 7.4) at 25°C. The stability of the individual ArPKD wild-type and mutant domains was determined by urea denaturation, using standard techniques (Pace 1986). The protein was incubated for 3h in varying concentrations of denaturant, and unfolding was monitored by change in intrinsic fluorescence using an Aminco Bowman fluorescence spectrometer with an excitation of 280 nm and emission monitored at the wavelength of maximum emission (320nm for W36C and 350 – 360nm for wild type and all other mutants). The raw data were fitted to a standard two state equation, which allows $[\text{urea}]_{50\%}$ (the concentration of denaturant where 50% of the protein is denatured) and the *m*-value (the dependence of $\Delta G_{\text{D-N}}$ on the concentration of urea) to be determined. **Figure 7** shows a representative recording of the change in fluorescence vs. concentration of urea: where $[\text{urea}]_{50\%}$ is the concentration of denaturant where 50% of the protein is denatured, and *m* is the dependence of $\Delta G_{\text{D-N}}$ on the concentration of urea. The PCPMer software package was used to analyze protein sequence alignments of related proteins to detect conserved physical-chemical properties (Mathura *et al.* 2003; Garcia *et al.* 2009).

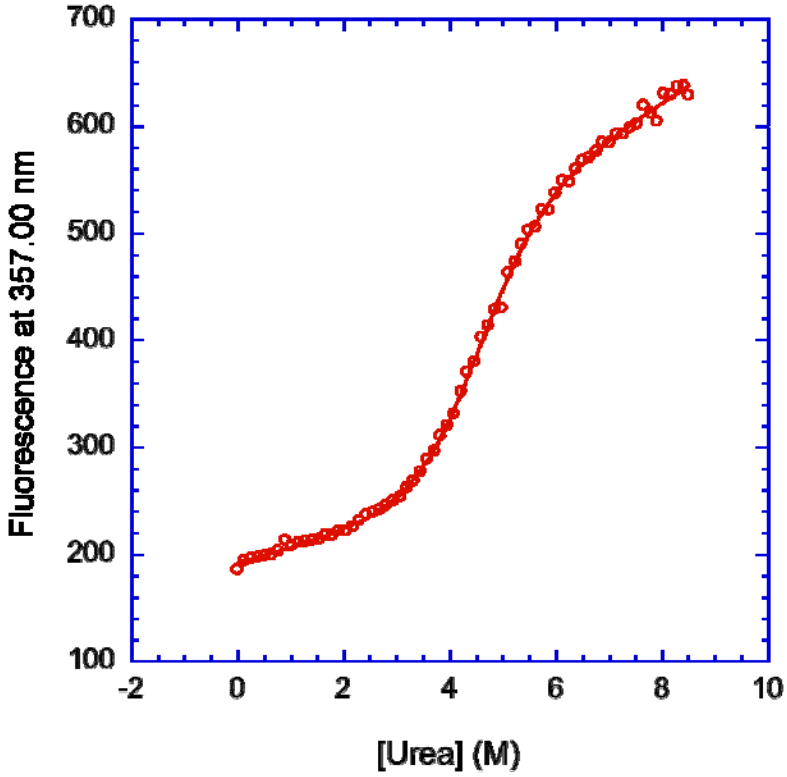

Figure 7: **Change in fluorescence of wild-type ArPKD vs. denaturant concentration.** The free energy for unfolding in 0M denaturant ($\Delta G_{\text{D-N}}^{H_2O}$) can be calculated from $\Delta G_{D-N}^{H_2O} = m[\text{urea}]_{50\%}$ [equation 1]

3.2.5 Determining equivalent mutations in an archaea PKD domain

The solved structures of the HuPKDd1 (Protein Data Bank (PDB) code 1B4R) and the ArPKD (PDB code 1L0Q) domain were visualized using Insight II, a commercially available program that allows structures to be manipulated and visually superimposed, and the structures were compared to determine which residues were spatially best aligned. From this alignment, it was possible to determine where to make the mutations in ArPKD that would be most nearly equivalent to those in the PC1 PKD domains.

3.3 RESULTS

3.3.1 Multiple sequence alignment of the PC1 PKD domains and location of naturally occurring missense mutations

The NMR structure of the first PKD domain (HuPKDd1) shows that it has a beta-sandwich structure with two sheets that pack together with a well defined hydrophobic core, centered around a conserved tryptophan located in the C strand (Bycroft *et al.* 1999). PC1 contains 16 homologous PKD domains. **Figure 8A** shows a sequence alignment of the 16 domains, together with an analysis of conserved motifs. The alignment and motif detection was done by using the PCPMer program (Garcia *et al.* 2009). This program automatically detects sequence motifs defined in terms of the conserved physical-chemical properties of residues in protein families. There are six conserved motifs in PC1 PKD domains (highlighted in *gray*). There are about 40 missense mutations that result in non-conservative amino acid substitutions involving residues that form part of PKD domains (highlighted in *cyan*). Interestingly, most of these mutations (30 out of 40) are found in conserved regions.

3.3.2 Selections of the missense mutations on PKD domains

Of these missense mutations, we selected six (**Figure 8A**) because these have been assigned as likely to be pathogenic. These are listed in **Table 1**. The first mutation targets PKD domain 1 where a charged amino acid (Arg) is changed to a hydrophobic amino acid (Leu); the same position in the *Fugu rubripes* PKD domain 1 is occupied by a basic residue (Sandford *et al.* 1997; Thomas *et al.* 1999). The second mutation targets the conserved Trp in PKD domain 3 (changed to an Arg), which results in a pathogenic phenotype (Rossetti *et al.* 2007). The third mutation also occurs in PKD domain 3 and changes a polar amino acid (Gln) to His. Interestingly, the mutated glutamine is conserved in PKD domain 3 from *F. rubripes* to human (Sandford *et al.* 1997; Burtey *et*

al. 2002). The fourth mutation is found in PKD domain 5 within the CC' loop region. The mutation occurs within the most conserved sequence of the PKD domains, WDFGD**G**S (Bycroft *et al.* 1999). This sequence is conserved from archaea to humans (**Figure 8B**). The glycine that is replaced (in bold) is in the C – C' turn. Its replacement by the bulkier serine is very likely to disrupt this structure (Phakdeekitcharoen *et al.* 2000). The fifth mutation is a replacement of two amino acids (Phe and Thr) to Leu. This is a large change that is likely to be pathogenic (Rossetti *et al.* 2001). The last mutation is found in PKD domain 16 where a Tyr is replaced by a Cys. This mutation was found to be pathogenic (Rossetti *et al.* 2003).

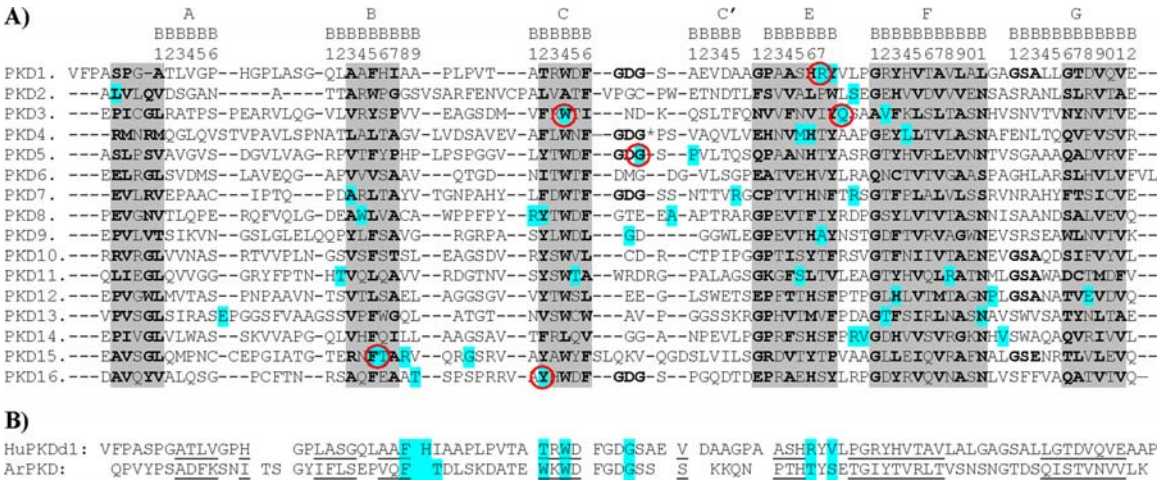

Figure 8: **Sequence alignment of PKD domains. A)** multiple sequence alignment of the 16 human PKD domains with structural motifs *highlighted*. The alignment and motif detection was done by using PCPMer program (Mathura *et al.* 2003). This program automatically detects sequence motifs defined in terms of the conserved physical-chemical properties of residues in protein families. The missense mutations are highlighted in *cyan*, and the selected for this work are *circled in red*. PKD4 has additional residues in the CC_ loop. *, EQALHQFQPPYNESFPVPD. **B)** structure-based sequence alignment of the first human PC1 PKD domain (HuPKDd1) and archaeal PKD domain (ArPKD) and location of pathogenic mutation positions. The best aligned residues are *underlined*. The equivalent positions of missense mutations in both domains are highlighted (in *cyan*).

Table 1: List of pathogenic missense mutations in human PC1 PKD domains and equivalent residues in HuPKDd1 and ArPKD

Residue Number	PKD domain number	Mutation position in HuPKDd1	Mutation position in ArPKD	Location strand	Surface /core
Arg-324 → Leu	1	R57L	T54L	E	surface
Trp-967 → Arg	3	W38R	W38R	C	core
Gln-987 → His	3	V59H	S56H	E-F loop	surface
Gly-1166 → Ser	5	G43S	G43S	C-C' loop	short loop
Leu-1992, Thr-1993 FT→Leu	15	FH26L	FT26L	B	Surface, core
Tyr-2092 → Cys	16	T36C	W36C	C	core

3.3.3 Effect of mutations on thermodynamic stability of PKD domains

We wanted to compare the effects of the selected point mutations on the thermodynamic stability of HuPKDd1. However, this domain is only marginally stable (~1 – 2 kcal mol^{-1} (12)), so it is difficult to get accurate stability data. However, it has been previously shown that it is possible to use homologous domains to model the effects of pathogenic mutations in Ig-like domains (Randles *et al.* 2006). The PKD domain from *Methanosarcina* archaebacteria (termed ArPKD) (Jing *et al.* 2002) has a very similar structure to HuPKDd1 (the two structures superimpose with an root mean square deviation of 2.2 Å (Jing *et al.* 2002)) but is thermodynamically more stable (4.4 kcal mol^{-1}). ArPKD therefore presents itself as a good model system to study pathogenic mutations in PC1 PKD domains. To make equivalent mutations in the human PKD and ArPKD domains, the best approach was to examine the published structures (Bycroft *et al.* 1999; Jing *et al.* 2002) and create an alignment of the two sequences. The results of this analysis are shown in **Figure 8B**, a structure-based alignment of the ArPKD and HuPKDd1 amino acid sequences. The *underlined* sections of the sequence are the best aligned structurally. From this alignment, it was possible to determine where to make the mutations in ArPKD that would be most nearly equivalent to those in the PC1 PKD

domains. The sites of the mutations in the aligned sequence are highlighted in *cyan* in **Figure 8B** and are listed in **Table 1**. In equilibrium denaturation experiments, unfolding was monitored by following changes in intrinsic tryptophan fluorescence. The results are shown in **Figure 9**, and the results are summarized in **Table 2**. The mutants FT26L and W38R were unfolded in buffer. All point mutations destabilize the ArPKD domain to some extent.

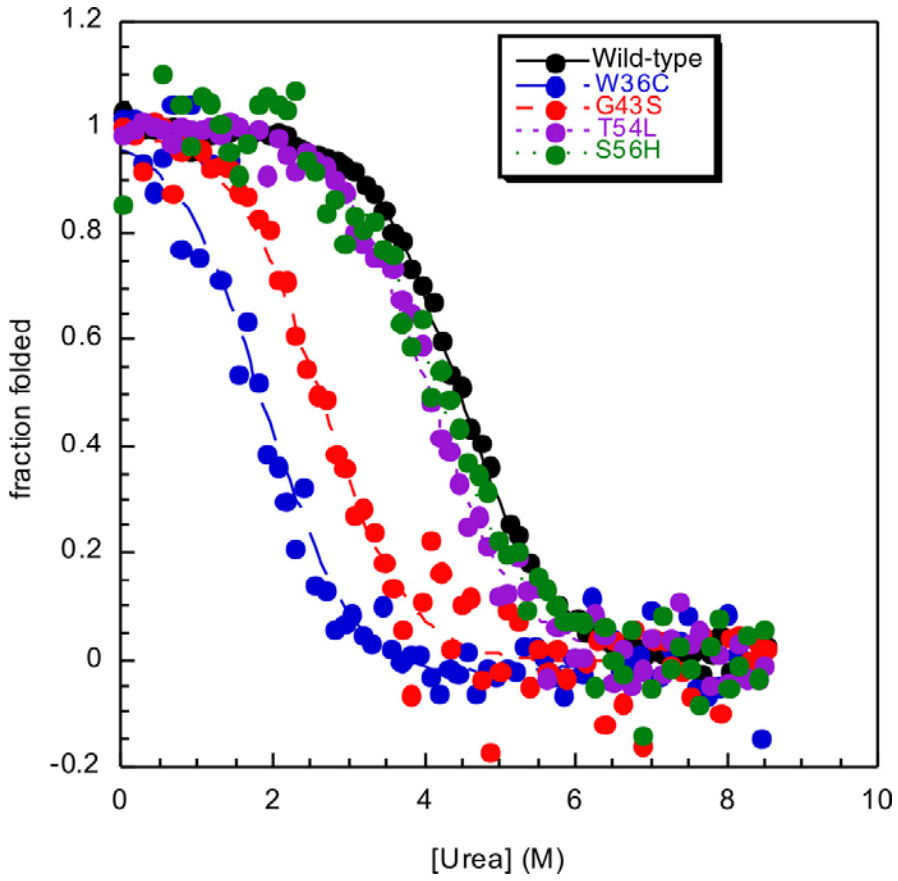

Figure 9: **Equilibrium denaturation curves for ArPKD mutants.** The effects of missense mutations T54L, S56H, G43S, and W36C on ArPKD domain stability are shown. All four mutants are made to model pathogenic mutations in HuPKDd1 domains. It is clear from the changes in the midpoint that both W36C and G43S destabilize the domain significantly, whereas the mutations T54L and S56H have little effect on the stability of the PKD domain.

Table 2: Thermodynamic stabilities of ArPKD mutants

Mutation Position in ArPKD	*m*-value	$[urea]_{50\%}$ ArPKD	$\Delta G_{D\text{-}N}^{H_2O}$ ArPKD
	($kcal\ mol^{-1}\ M^{-1}$)	(M)	($kcal\ mol^{-1}$)
Wild type	1.0 ± 0.1	4.4 ± 0.1	4.4 ± 0.1
T54L	1.0 ± 0.1	4.1 ± 0.1	4.1 ± 0.1
W38R	Unfolded	n/a	n/a
S56H	0.9 ± 0.1	4.5 ± 0.1	4.1 ± 0.1
G43S	1.0 ± 0.1	2.6 ± 0.1	2.6 ± 0.1
FT26L	Unfolded	n/a	n/a
W36C	1.0[α]	1.9 ± 0.1	1.9 ± 0.1

[a] Because W36C was so destabilized that there was no true folded baseline, the data were fitted with *m* fixed to the wild-type value of 1.0.

3.3.4 Effects of missense mutations on the mechanical stability of HuPKDd1

To study the effect of missense mutations on the mechanical stability of PKD domains, we used HuPKDd1 as a template because its structure is known (Bycroft *et al.* 1999) and its thermodynamic and mechanical stabilities have been characterized (Forman *et al.* 2005; Qian *et al.* 2005). To make equivalent mutations in the HuPKDd1 domain, we used the sequence alignment shown in **Figure 8** and mutated the equivalent residues using site-directed mutagenesis. The locations of the different residues mutated in HuPKDd1 are shown in **Figure 10**.

For example, the change of Val-59 to His in HuPKDd1 corresponds to the natural mutation Gln-987 to His in PKD domain 3. We used a heteropolyprotein approach to study the mechanical properties of mutant HuPKDd1 domains using single-molecule AFM techniques. In these constructs, we used the titin domain I27 as an internal mechanical fingerprint that has been extensively studied with AFM techniques (Carrion-Vazquez *et al.* 1999; Li *et al.* 2002). Also, I27-based protein chimeras have been found to express well in bacteria; this strategy has proven to be useful in the analysis of several protein domains with single molecule AFM (Best *et al.* 2001; Oberhauser *et al.* 2002; Steward *et al.* 2002; Li *et al.* 2005; Brucale *et al.* 2009).

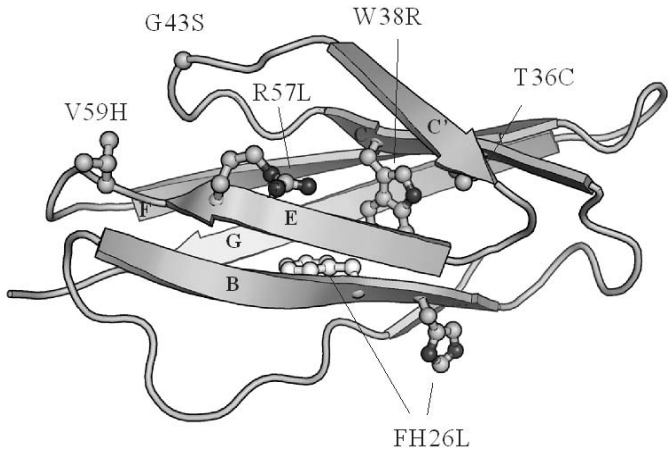

Figure 10: NMR structure of HuPKDd1 showing the positions of mutated residues. The figure was prepared using the program PyMOL.

Figure 11 shows typical examples of force-extension curves obtained for I27 heteropolyproteins harboring the wild-type and mutant HuPKDd1. As shown before, the wild-type HuPKDd1 has a mechanical stability very similar to I27 domains and unfolds at forces of about 180 pN (**Figure 11F**) (Forman *et al.* 2005; Qian *et al.* 2005) . **Figure 11, B – E**, shows that missense mutations R57L, V59H, G43S, and T36C all result in a significant decrease in the mechanical stability. For example, the R57L mutant domain unfolds at forces of ~140 pN (**Figure 11G**), which is seen as the force peaks (marked in **Figure 11B** by the *dashed line*) preceding the unfolding of the I27 domains (they unfold at ~180 pN). The G43S mutation has a strong destabilizing effect on HuPKDd1. This mutant domain unfolds at ~55 pN, which is seen as a small force peak (marked by the *arrow*) preceding the unfolding of the I27 domains (**Figure 11D**).We found that the W38R and FT26L mutations severely destabilize the PKD domain because we were not able to express these constructs as soluble proteins.

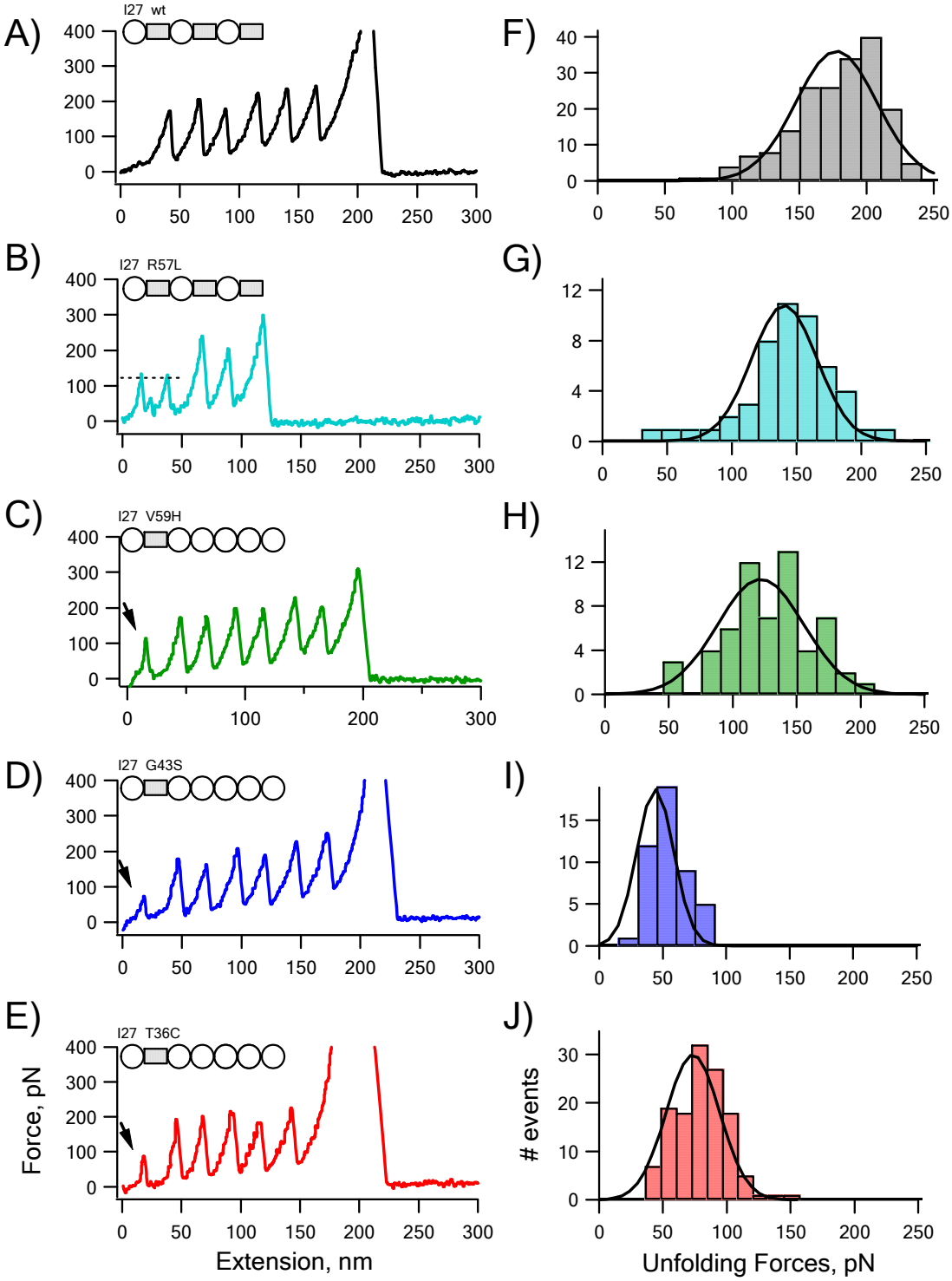
A)
I27 wt
B)
I27 R57L
C)
I27 V59H
D)
I27 G43S
E)
I27 T36C
Force, pN
Extension, nm
F)
G)
H)
I)
J)
events
Unfolding Forces, pN

Figure 11: Force-extension relationships for wild type and mutant HuPKDd1 measured with AFM techniques. Stretching single molecule of each construct gave force-extension curves that followed a saw-tooth pattern with equally spaced force peaks. The cartoon above each recording shows the construction of each recombinant protein chimera. The wild type HuPKDd1and the R57L mutant were constructed by repeating the I27-HuPKDd1 three times. The T36C, G43S and V59H HuPKDd1 mutants were flanked by several I27 domains (to increase the solubility of expressed protein). The dashed lines in **A**) and **B**) present the average force used to unfold either wild type or R57L mutant HuPKDd1. The force peaks pointed by solid arrow represent the unfolding of mutant domains of V59H (**C**), G43S (**D**) and T36C (**E**). The forces used to unfold the wild type and mutated HuPKDd1 are shown as a force histogram. The force peaks of wild type PKD had an average force of 176±32pN (n=189). The average forces for unfolding the HuPKDd1 mutants are: 143±34pN (n=50) for R57L, 127±33pN (n=59) for V59H, 54±15pN (n=46) for G43S and 79±20pN (n=129) for T36C. All the experiments were carried out at the pulling speed of 0.4-0.6nm/ms.

3.3.5 Kinetics of unfolding of HuPKD1 mutants

To quantify the effect of the missense mutations on the kinetics of unfolding, we analyzed the effect of pulling speed on the unfolding forces. **Figure 12** shows a plot of the average unfolding force *versus* the pulling rate for wild type and different mutants. The parameters used for the Monte Carlo simulation are shown in **Table 3**. The unfolding rate constants, α_o, of the four mutants are higher than that of the wild type (9.8×10^{-4} s^{-1}), indicating that the activation energy of unfolding was decreased by the mutations. The unfolding distances to the transition state, x_u, of the G43S and T36C mutants are also larger than the wild type, indicating that there is a significant change in the unfolding pathway.

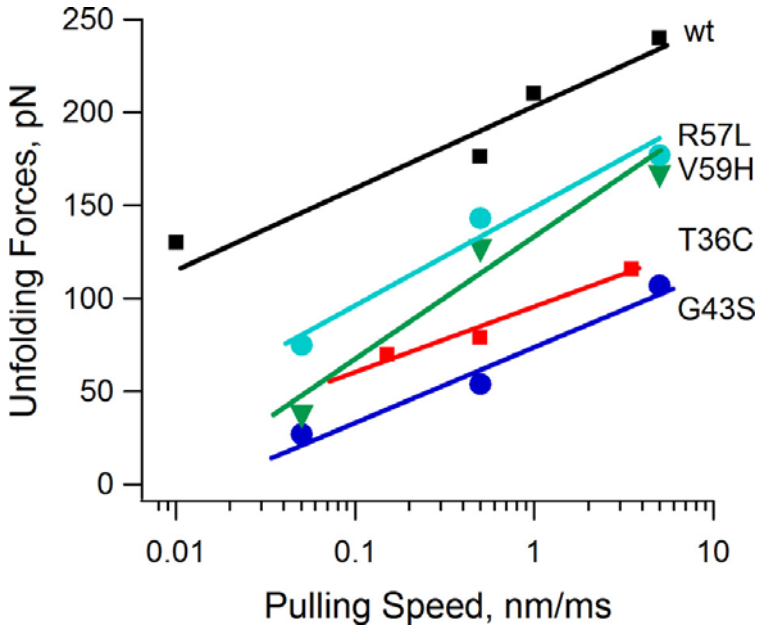

Figure 12: Kinetics of unfolding of HuPKDd1 mutants. A plot of the average unfolding force *versus* the pulling rate for wild-type (*wt*, *black squares*), R57L (*cyan circles*), V59H (*green triangles*), T36C (*red squares*), and G43S (*blue circles*) HuPKDd1 domains is shown. The *solid lines* are fits of the Monte Carlo simulation to the experimental data (see "Experimental Procedures"). The parameters used for the Monte Carlo simulation are shown in Table 3.

Table 3: Estimated mechanical kinetic parameters of HuPKDd1 mutants

	F_u [a]	α_o	x_u
	pN	s^{-1}	*nm*
Wild type	176 ± 32	$9.8 \pm 8.1 \times 10^{-4}$	0.25 ± 0.02
R57L	143 ± 34	$2.6 \pm 1.8 \times 10^{-2}$	0.24 ± 0.01
V59H	127 ± 33	$6.9 \pm 5.3 \times 10^{-2}$	0.22 ± 0.01
G43S	54 ± 15	$2.3 \pm 1.8 \times 10^{-1}$	0.31 ± 0.02
T36C	79 ± 20	$0.7 \pm 0.5 \times 10^{-1}$	0.32 ± 0.02

[a] At pulling speed of 0.4-0.6 nm ms^{-1}.

3.4 DISCUSSION

We used HuPKDd1 as a model system for assessing the effects of mutation on the mechanical stability of PKD domains in general. In general, we found that all the mutations resulted in a loss in mechanical stability. A number of studies have demonstrated that homologous proteins have the same unfolding pathways on application of force, *i.e.* the same mechanisms for resisting forced unfolding. Using a combination of simulations and experiments, we have recently shown that the same is true of HuPKDd1 and ArPKD. 5 Hence, mutations that promote mechanical unfolding in HuPKDd1 are likely to have the same effect in other PKD domains.

3.4.1 All the mutations destabilize HuPKD and ArPKD domains to some extent

Table 4 shows a summary of the effects of missense mutations on HuPKDd1 and ArPKD.

Table4: Effects of missense mutations on HuPKDd1 and ArPKD

Mutation Position in HuPKDd1	Mutation Position in ArPKD	$\Delta\Delta G_{\text{D-N}}^{H_2O}$ ArPKD	ΔF_u HuPKDd1
		kcal mol^{-1}	*pN*
wild type	n/a	--	--
R57L	T54L	0.3 ± 0.1	33
W38R	W38R	>4.4	n/a
V59H	S56H	0.3 ± 0.1	49
G43S	G43S	1.8 ± 0.1	122
FH26L	FT26L	>4.4	n/a
T36C	W36C	2.5 ± 0.1	97

[a] Because W36C was so destabilized that there was no true folded baseline, the data were fitted with *m* fixed to the wild-type value of 1.0.

3.4.2 Unfolded mutants

The FH26L (or FT26L in ArPKD) and W38R mutations result in an unfolded protein domain. This is not unexpected because these target large buried residues. In

particular, the Trp to Arg mutation, introducing a charged group into a buried position, causes a drastic reduction in stability. Furthermore, the tryptophan in that position is very highly conserved across the PKD domains, suggesting that it may have an importance for folding. Hence, for the W38R and FH26L, it seems very likely that the presence of the unfolded domain causes the observed disease phenotype. Perhaps the destabilized ectodomain of PC1 cannot perform its mechanosensing function, or perhaps the presence of the unfolded domain causes the protein to aggregate, to fail to be trafficked correctly, or to be degraded by the normal cell degradation machinery.

3.4.3 Destabilizing mutations

Mutation T36C (or W36C in ArPKD) to cysteine replaces a large surface aromatic with a small polar side chain. This is a position with a high degree of conservation in the PKD domains. Of the other 16 PKD domains, eight have a tyrosine and four have a phenylalanine at the equivalent position, all large aromatic side chains. Rossetti *et al.* (Rossetti *et al.* 2002) note that this residue is conserved in the C strand of many PKD domains, including in the mouse gene, but interestingly, in *F. rubripes*, there is a cysteine at the equivalent position. The G43S replaces a glycine with a serine in a loop region of the protein structure. This results in a significant destabilization. This destabilization might be expected, given the conservation in this region of the structure in PKD domains of polycystin. Interestingly, this glycine residue occupies a region Φ/ψ space of the Ramachandran plot (Ramachandran *et al.* 1963), which is disallowed for residues other than glycine (positive Φ, negative ψ) in the structures of both ArPKD and HuPKDd1. The T36C and G43S mutants had a very significant effect on the ability of HuPKDd1 to resist forced unfolding. The unfolding force is significantly lower in these mutants, and furthermore, the distance to the transition state (x_u) is significantly larger for

each of these mutants, suggesting that the unfolding pathway changes significantly. Such a change in x_u, associated with a change in folding mechanism, has been observed for mutants of I27 domain from human titin (Li *et al.* 2000). We conclude that mutations in these positions might potentially have a significant effect on the mechanical function of PC1.

3.4.4 Slightly destabilizing mutations

The mutations that are only slightly destabilizing, R57L and V59H (T54L and S56H in ArPKD), are surface mutations. This suggests that these mutations are in regions of the protein that are not important for the mechanical stability of the PKD domains. Thomas *et al.* (Thomas *et al.* 1999) reported the R57L mutation. They note the change from a basic to neutral hydrophobic residue and report that this is the only PKD domain with a basic residue in this position. Furthermore, a basic residue is found in the equivalent position in *F. rubripes*. Due to this conservation, they suggest that this residue may be functionally important, for example, in ligand binding or protein- protein interactions (Thomas *et al.* 1999). Our results do not suggest that this is a position that is critical for the mechanical stability of PKD domains.

3.4.5 Conclusions

These data suggest that the effect of the mutations G43S, T36C, and in particular, W38R and FH26L are likely to be mainly due to the large destabilization these mutations confer on the parent PKD domain (*i.e.* G1166S, Y2092C, W967R, and F1992L, T1993L, respectively). They will also, therefore, compromise the ability of PC1 to act as a mechanosensor. In time, it may be possible to analyze naturally occurring variations in the genome sequence, predict the biophysical effect of the mutation, and estimate the likelihood of a given variation to be deleterious or benign. As seen here, such studies

could also suggest further research into protein function, and possibly, mutation-specific therapies. There is increasing interest in human protein mutations, particularly naturally occurring mutations that may be disease-related. Although many of these proteins are experimentally intractable, the strategy presented here could make mutation studies in many human proteins possible for the first time.

Chapter 4

Naturally Occurring Osmolytes Modulate the Mechanical Properties of PKD Domains

4.1 INTRODUCTION

Many proteins are found in harsh environments such as in the kidney. Polycystin-1 (PC1) is a large membrane protein that has a long N-terminal extracellular region with a multi-modular structure including sixteen Ig-like polycystic kidney disease (PKD) domains which are exposed to urea and other osmolytes. Urea is known as a common denaturant that affects proteins function by destabilizing their structure (Pace 1975). On the other hand, it is know that the native conformation of proteins can be stabilized by naturally occurring osmolytes (such as TMAO, betaine, sucrose, trehalose, sarcosine, sorbitol, proline and glycerol (Street *et al.* 2006)), which are found in the kidneys of elasmobranches to humans (Yancey *et al.* 1982; Garcia-Perez *et al.* 1991; Schmolke *et al.* 1996; Venkatesu *et al.* 2009). The distribution of osmolytes in mammalian kidneys shows a generally increasing pattern along their corticomedullary axes. For example, sorbitol, glycerophosphorylcholine (GPC) and betaine usually reach to a maximum level at the tip of the papilla where collecting ducts are found (Garcia-Perez *et al.* 1991).

The mechanisms by which osmolytes promote protein folding, increase protein stability and induce conformational changes have been the focus of intensive investigation (Baskakov *et al.* 1998; Kumar *et al.* 1999; Bolen 2001; Ratnaparkhi *et al.* 2001; Zou *et al.* 2002; Auton *et al.* 2005; Ignatova *et al.* 2006; Street *et al.* 2006; Beck *et al.* 2007; Loo *et al.* 2007; Street *et al.* 2009; Venkatesu *et al.* 2009); however, most of these studies have been limited to the study of thermodynamic stability by using ensemble denaturation experiments or molecular dynamic simulations. Little is known

about the influence of osmolytes on the mechanical stability of modular proteins, especially the ones with mechanosensing functions.

Here single-molecule AFM is used to test the effects of various naturally occurring osmolytes on the mechanical properties of PKD domains. This experimental approach more closely mimics the conditions found *in vivo*. The results demonstrate that TMAO, sorbitol and sarcosine effectively counteract the destabilizing effects of urea by restoring the normal mechanical properties of PKD domains. The data suggest that the mechanosensing properties of PC1 are modulated by interplay of urea and protecting osmolytes.

4.2 Materials and Methods

4.2.1 Reagents and buffers used in osmolyte experiments

1. MilliQ H_2O (18.2 MΩ)
2. Phosphate buffered saline (PBS) (Sigma-Aldrich) with 137mM NaCl, 2.7mM KCl, 10mM sodium phosphate dibasic, 2mM potassium phosphate monobasic and a pH of 7.4
3. Urea (Fisher Scientific); guanidinium chloride (GdmCl) (Fluka, Sigma-Aldrich);
4. TMAO (Fluka, Sigma-Aldrich);
5. Sorbitol (Sigma-Aldrich); sarcosine (Sigma-Aldrich); all of these were 99% pure.

4.2.2 Surfaces for AFM experiments

The preparation of glass, silanized glass and Ni-NTA coverslips followed the protocols in chapter 2.

4.2.3 Cantilevers for AFM Experiments

Three types of cantilevers were used in osmolytes experiments: MLCT, MSNL and OBL-105 (MLCT-AUHW, Veeco Metrology Group, Santa Barbara, CA). Calibration followed section 2.2.7.

4.2.4 Cloning, expression and purification of PolyPKDd1-I27, PolyI27 and PolyArPKD proteins for AFM experiments

PolyPKDd1-I27 ((I27-HuPKDd1)$_3$-I27) and polyI27 ((I27)$_8$) polyproteins were cloned and expressed in *Escherichia coli* cells following the protocols in Chapter 2. PolyArPKD containing seven identical repeats of ArPKD domain was constructed using a multiple-step cloning technique (Steward *et al.* 2002; Forman *et al.* 2009), and then the protein was expressed in *Escherichia coli* C41 strain. Proteins were purified by Ni-affinity chromatography as previously described (Carrion-Vazquez *et al.* 1999; Forman *et al.* 2005; Qian *et al.* 2005; Ma *et al.* 2009) and stored in PBS containing 5mM DTT at 4 °C.

4.2.5 Single-molecule atomic force microscopy

The mechanical properties of the proteins were studied using a home-built single molecule AFM as previously described in Chapter 1. In order to minimize the variation in the calibration of cantilever in different aqueous systems, each individual cantilever was calibrated in PBS buffer. The pulling speed was in the range of 0.5-0.7 nm/ms.

4.2.6 Single protein mechanics in osmolytes

In AFM experiments, a small aliquot of the purified proteins was first adsorbed onto a substrate, e.g. Ni-NTA coated glass coverslips (Itoh *et al.* 2004; Sakaki *et al.* 2005). The unbinding proteins were rinsed off with PBS. The effects of osmolytes on mechanical stability of proteins were studied by using the combination of AFM and

buffer substitution. The tested buffers were PBS (control), denaturants at different concentrations, protecting osmolytes, and different mixtures of denaturants and protecting osmolytes. Due to the weakening effect of osmolytes on the binding affinity of protein to both cantilever and substrate, the pick-up efficiency was typically very low, making these experiments quite challenging.

4.2.7 Measuring the refolding rate of PKD domains

The refolding rate of PKD domains was investigated by using a double-pulse protocol as previously described (Carrion-Vazquez *et al.* 1999). When a polyprotein molecule is extended close to its contour length, the number of unfolded domains is counted as a total of available domains (N_{total}). Then the molecule is allowed to relax for a variable time intervals (t) before it is stretched again. The number of unfolding events observed in the second stretch is counted as the refolded domains ($N_{refolded}$). By stretching and relaxing one polyprotein molecule repeatedly, the fraction of refolded modules ($N_{refolded}$ / N_{total}) is measured with variable relaxation time (t). Polyprotein refolding is typically well described by a single exponential function $Pf_{(t)} = 1 - e^{-t\beta}$, where $Pf_{(t)}$ represents the probability of the refolding ($N_{refolded}$ / N_{total}), t represents time and β is the refolding rate (Carrion-Vazquez *et al.* 1999).

4.3 RESULTS

4.3.1 The mechanical stability of PKD domains is remarkably sensitive to the urea concentration

To study the effect of osmolytes on the mechanical stability of PKD domains, the first PKD domain from human PC1, i.e., PKDd1, was chosen since its structure is known (Bycroft *et al.* 1999) and its thermodynamic and mechanical stabilities have been characterized (Forman *et al.* 2005; Qian *et al.* 2005; Ma *et al.* 2009). A hetero-

polyprotein approach was used to study the mechanical properties of PKDd1, with titin I27 domain as an internal mechanical fingerprint.

Figure 13A shows the effects of the increase of urea concentrations on the stability of PKDd1 and I27 in polyPKDd1-I27 protein. At 0 M urea both domains unfolded at similar forces of ~190 pN (Forman *et al.* 2005; Qian *et al.* 2005; Ma *et al.* 2009). Increasing the urea concentration had a striking effect on the unfolding forces of PKDd1 but a relatively small effect on those of I27. For example, the unfolding pattern in 0.5 M urea showed a total of six force peaks (four at ~190 pN and two at ~100 pN), with the four high force peaks interpreted as the unfolding of I27 domains, given the structural design of polyPKDd1-I27 and external control of polyI27 (**Figure 13B**). This recording also shows that one of three unfolding events of PKD domains is 'missing'. By fitting the trace with the worm-like-chain equation (Bustamante *et al.* 1994; Marko *et al.* 1995) using an increase in contour length of 29 nm (red lines in **Figure 13A**), the spacer before the sawtooth pattern was measured as the contour length of a PKD domain, indicating it was already unfolded before stretching or unfolded at force that was below our detection limit (~20 pN). At 3 M urea all PKD domains were greatly destabilized or unfolded as evidenced by the long spacer before the unfolding of the I27 domains. As a control, polyI27 protein was used to study the effect of urea on I27 mechanical stability (**Figure 13B**). The data showed that urea had a very small effect on the mechanical stability of I27 domains; at 3 M urea the unfolding forces decreased by only 13% (from 190 pN to 180 pN).

We also observed other unfolding patterns when stretching the polyPKDd1-I27 protein in urea. For instance, **Figure 13C** shows that in 1 M urea the contour length of each PKD domain is 22 nm instead of 29 nm. This type of events accounts for about 15% of the total recordings. An increase in contour length of 22 nm corresponds to the

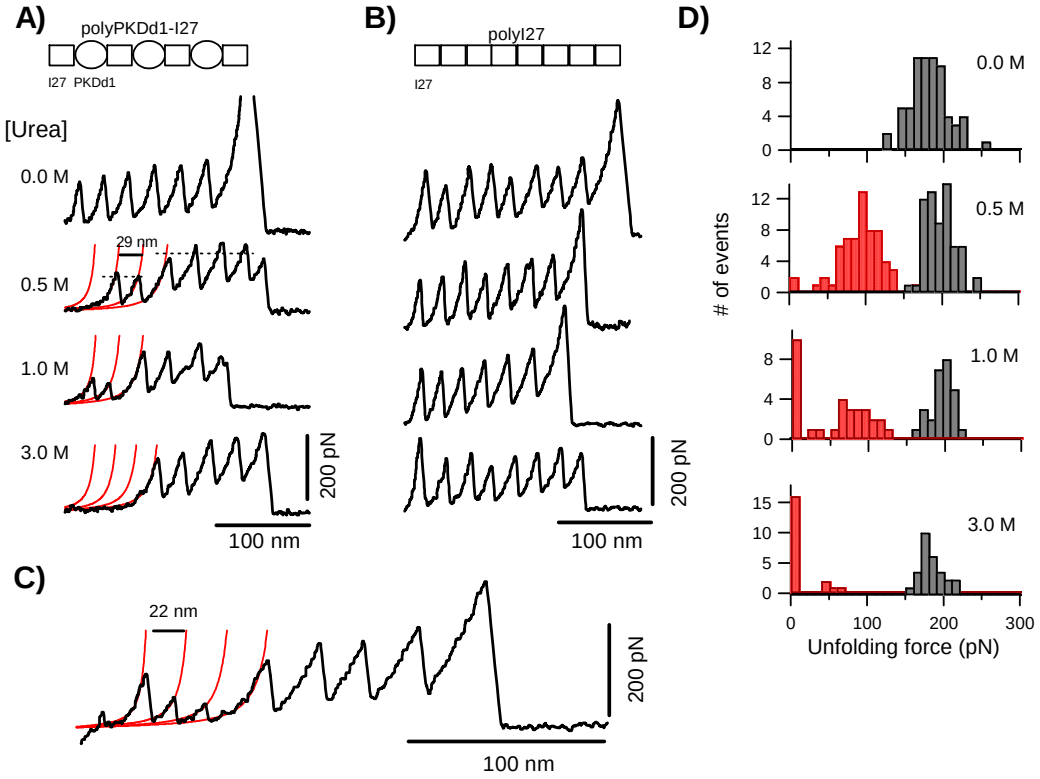

Figure 13: **Urea has a strong destabilizing effect on human PKD domains. A)** Force-extension curves of polyPKDd1-I27 proteins under increasing concentrations of urea (from 0 to 3 M) show the unfolding patterns of PKD and I27 domains. At 0 M urea both domains unfold at similar forces of about 190 pN (188 ± 25pN, n=67) whereas at 3 M urea PKD domains are all denatured with little effect on I27 domains. The red lines correspond to fits to the worm-like-chain equation. As shown in A) some PKD domains are "missing" from the unfolding pattern obtained under urea. **B)** Force-extension curves of polyI27 proteins under the same range of urea concentrations. **C)** Unfolding force histograms for the polyPKDd1-I27 protein at 0.0 M, 0.5 M, 1.0 M and 3.0 M urea. The missing unfolding events are counted as points below the noise level (~20 pN) in the histograms. The unfolding events for I27 and PKD domains in the polyPKDd1-I27 protein are shown as grey and red bars, respectively. The average unfolding forces for I27 and PKD domains are: 195 ± 19 pN (n=82) and 103 ± 28 pN (n=63) in 0.5 M, 187 ± 22 pN (n=27) and 78 ± 36 pN (n=31) in 1 M, 178 ± 18 pN (n=24) and <20 pN (n=19) in 3 M. **D)** Example of a force-extension curve of a polyPKDd1-I27 protein in 1 M urea showing partially folded PKD domains. The increase in contour length upon PKD domain unfolding is 22 nm instead of 29 nm.

unfolding of about 70 amino acids, suggesting that these PKD domains were partially unfolded in 1 M urea.

The effects of urea on polyPKDd1-I27 protein are quantified in **Figure 13D** and **Figure 14**. **Figure 13D** shows the histograms of unfolding force at 0 M, 0.5 M, 1 M and 3 M urea, respectively. At 0.5 M there is significant shift of the unfolding forces for PKD domains to about 100 pN (red bars, 96 ± 28 pN, n=63) but not for I27 domains (grey bars, 195 ± 19 pN, n=64). We found that the fraction of missing PKD domains increases as a function of urea concentration (8% in 0.5 M, 32% in 1 M and 76% in 3 M). **Figure 14** shows a plot that compares the effects of urea concentrations on the unfolding forces

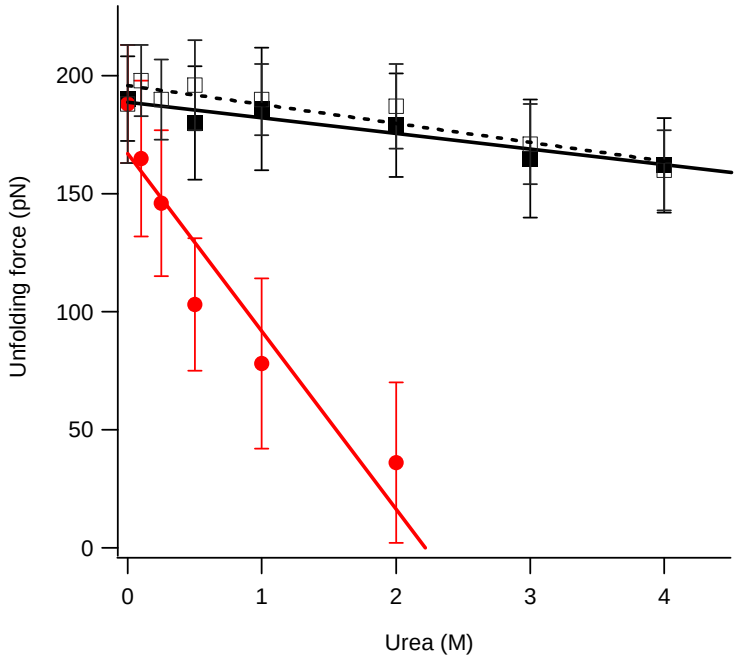

Figure 14: Comparison of the effects of urea on the mechanical stability of I27 and PKD domains. The unfolding forces for PKD (red circles) and I27 (black squares) domains in the polyPKDd1-I27 protein are plotted as a function of the urea concentration. The open squares correspond to the unfolding forces of I27 in the polyI27 protein. The lines are linear fits to the experimental data. The slopes are 7 pN/M for I27 and 75 pN/M for PKD domains, respectively.

of PKD domains (red circles) with those of I27 domains (black squares). Linear relationship was found between the mechanical stability and urea concentration for both domains; however, PKD domain has a steep slope of 75 pN/M, meaning that it is about ten-times more sensitive to urea than I27 domain (slope of 7 pN/M). These results indicate that urea at physiological concentrations (<1M) has a strong destabilizing effect on PKD domains.

4.3.2 Effects of protecting osmolytes on the mechanical stability of urea-weakened PKD domains

Several naturally occurring osmolytes have been shown to counteract the destabilizing effects of urea on several types of proteins. Based on these observations we hypothesized that osmolytes such as sarcosine, TMAO or sorbitol may offset urea destabilizing effects on PKD domains. **Figure 15** shows an experiment where polyI27-PKD proteins were first exposed to 1 M urea and then switched to a 1:1 mixture of 1 M urea and sorbitol (**Figure 15A**). The data show sorbitol has a striking stabilizing effect. In 1 M urea, most PKD domains are significantly destabilized. We found that in the presence of an equivalent concentration of sorbitol the unfolding forces of PKD domains were restored to the values in PBS.

Similar effects were observed when sorbitol was substituted with 1 M TMAO (**Figure 15A**) or 1 M sarcosine (data not shown), indicating that a 1 M osmolyte to 1 M urea ratio seems adequate to restore the mechanical stability of PKD domains in the presence of 1 M urea. In order to quantify the stabilization effect, we carried out mechanical unfolding experiments of polyPKDd1-I27 at different molar ratios of sorbitol and urea. In **Figure 15B**, it shows a plot of the mechanical stability, Fu, for PKD domains as a function of the ratio of sorbitol:urea. There is a linear increase in the mechanical stability at concentrations below 1 M sorbitol (of about 120 pN/M sorbitol).

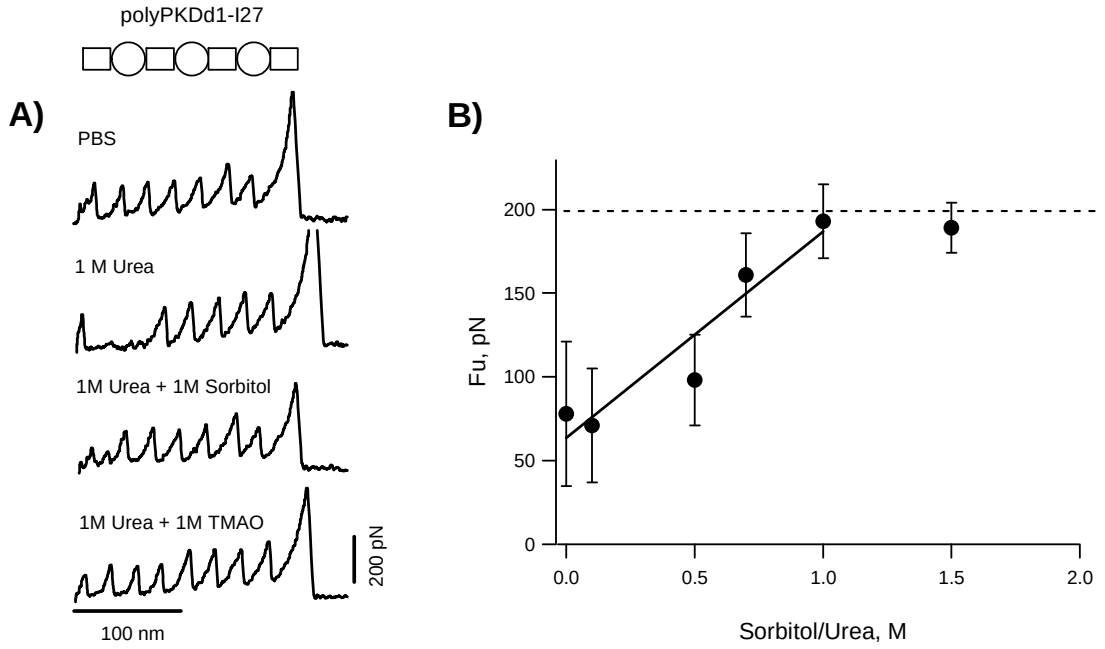

Figure 15: Sorbitol and TMAO counteract the destabilizing effects of urea on PKD domains. A) Typical force-extension traces of the polyPKDd1-I27 protein obtained in PBS, 1M urea, 1M urea + 1M sorbitol and 1M urea + 1M TMAO. **B)** Plot of the unfolding forces for PKD domains as a function of the ratio sorbitol:urea. There is a linear increase in the mechanical stability at concentrations below 1M sorbitol (of about 120 pN/M sorbitol).

4.3.3 Effects of osmolytes on the refolding rate of PKD domains

Another important parameter of mechanical property of a protein is its refolding rate. In order to estimate the refolding rate of PKD domains in PBS we used a double-pulse unfolding/refolding protocol (**Figure 16)**. A polyI27-PKDd1 molecule was first picked up and stretched close to its contour length and the total number of unfolded domains (N_{total}) was counted (six in this case) (**Figure 16A).** Based on the molecular design of this heteropolyprotein, these six unfolding events should result from the unfolding of three HuPKDd1 and three I27 domains. Then the unfolded polypeptide chain was relaxed quickly to zero force before a second stretch. After a five-second relaxation, only three domains unfolded in the second pull indicating that three out of six

domains refolded in five seconds (N_{ref}). These three refolded domains were interpreted as I27 domains based on the fact that they are known to refold within 5 seconds (Carrion-Vazquez *et al.*, 1999; **Figure 16B**). No refolded HuPKDd1 domains were detected during this time interval. We found that we had to wait as long as 20s to observe HuPKDd1 refolding. Interestingly, the mechanical stability was much lower than in the control first pulse (~ 50 pN; **Figure 16A**). This indicates that it took ~20 s for the HuPKDd1 domains to collapse and form a folded domain but with a much lower mechanical stability. This inefficient and sluggish refolding of the HuPKDd1 makes it impractical to study the effects of osmolytes using AFM techniques. For these reason we used a polyprotein made of a different PKD domain: an ArPKD domain.

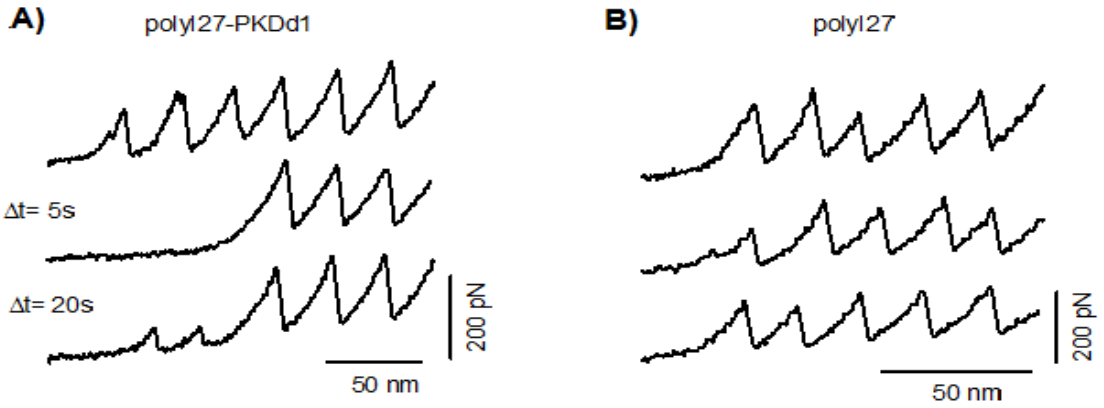

Figure 16: Measuring the refolding rate of HuPKD and I27 domains using a two-pulse stretching/relaxation protocol. Three consecutive force-extension are shown obtained with time delays of 5 s and 20 s for a HuPKD-I27 (A) and I27 polyprotein (B). I27 domains readily refold after mechanical denaturation whereas HuPKD domains do not.

4.3.4 Effects of chemical denaturants on the mechanical stability of an archaea PKD domain

The PKD domain from *Methanosarcina* archaebacteria (termed ArPKD) has a very similar structure to human PKDd1 (the two structures superimpose with an rmsd of

2.2 Å, (Jing *et al.* 2002)). Interestingly, as recently demonstrated by Forman *et al.*, both ArPKD and PKDd1 domains have a similar mechanical design and stability (they unfold at ~200 pN) (Forman *et al.* 2009). In addition, we found that naturally occurring missense mutations alter the thermodynamic stability of ArPKD and the mechanical stability of PKDd1 to a similar extent (Ma *et al.* 2009). Because of these similarities we decided to study the effects of urea on the mechanical stability of ArPKD For these experiments we used a polyprotein which has seven identical repeats of the ArPKD domain (1L0Q.pdb). Surprisingly, we found that urea as high as 3 M had a relatively small effect on the unfolding forces (a decrease of only ~50 pN). For this reason, we chose the more powerful denaturant guanidinium chloride (GdmCl). GdmCl is known to denature proteins at about 2-3 times lower concentrations as compared to urea (Greene *et al.* 1974; Colonna *et al.* 1978). **Figure 17** shows typical force-extension traces for the polyArPKD protein obtained at different GdmCl concentrations. Upon increasing the concentrations we observe a systematic decrease in the unfolding forces for ArPKD domains. For example, in 1 M the unfolding forces drop by 48 pN (from 189 ± 23 pN, n=64 to 141 ± 22 pN, n=71; **Figure 17B**). Therefore, in these experiments, GdmCl is about three times more effective in destabilizing ArPKD than urea.

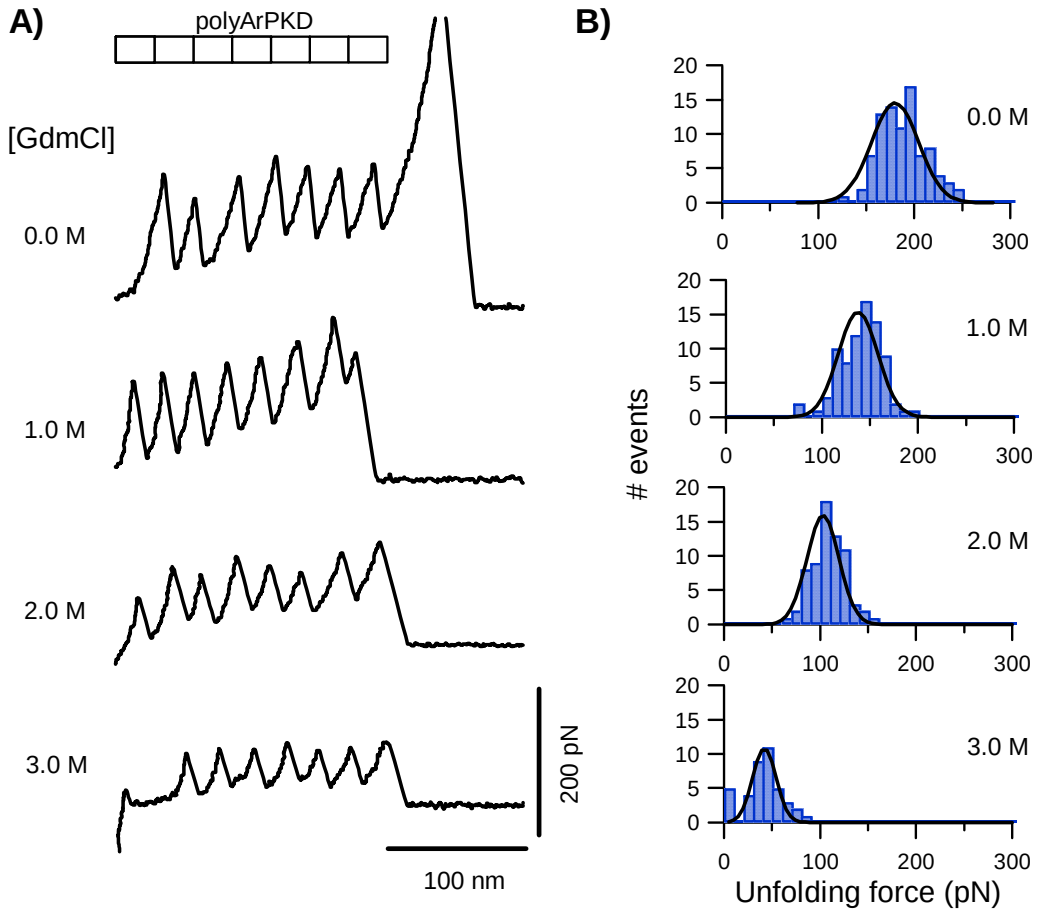

Figure 17: Effects of a chemical denaturant on the mechanical stability of an archaea PKD domain. A) Force-extension curves of polyArPKD proteins under increasing concentrations of GdmCl (from 0 to 3 M). Upon increasing the concentration there is a decrease in the unfolding forces for ArPKD domains, as shown in the histograms in **B)**.

4.3.5 Effects of osmolytes on the refolding rate of an archaea PKD domain

Using a double-pulse protocol we found that ArPKD domains readily refold (**Figure 18A**). The recovery from the unfolded state follows an exponential time course with a time constant of about 600 ms (**Figure 18B**). I then tested the effects of adding chemical denaturants and protecting osmolytes (**Figure 18C, D).**

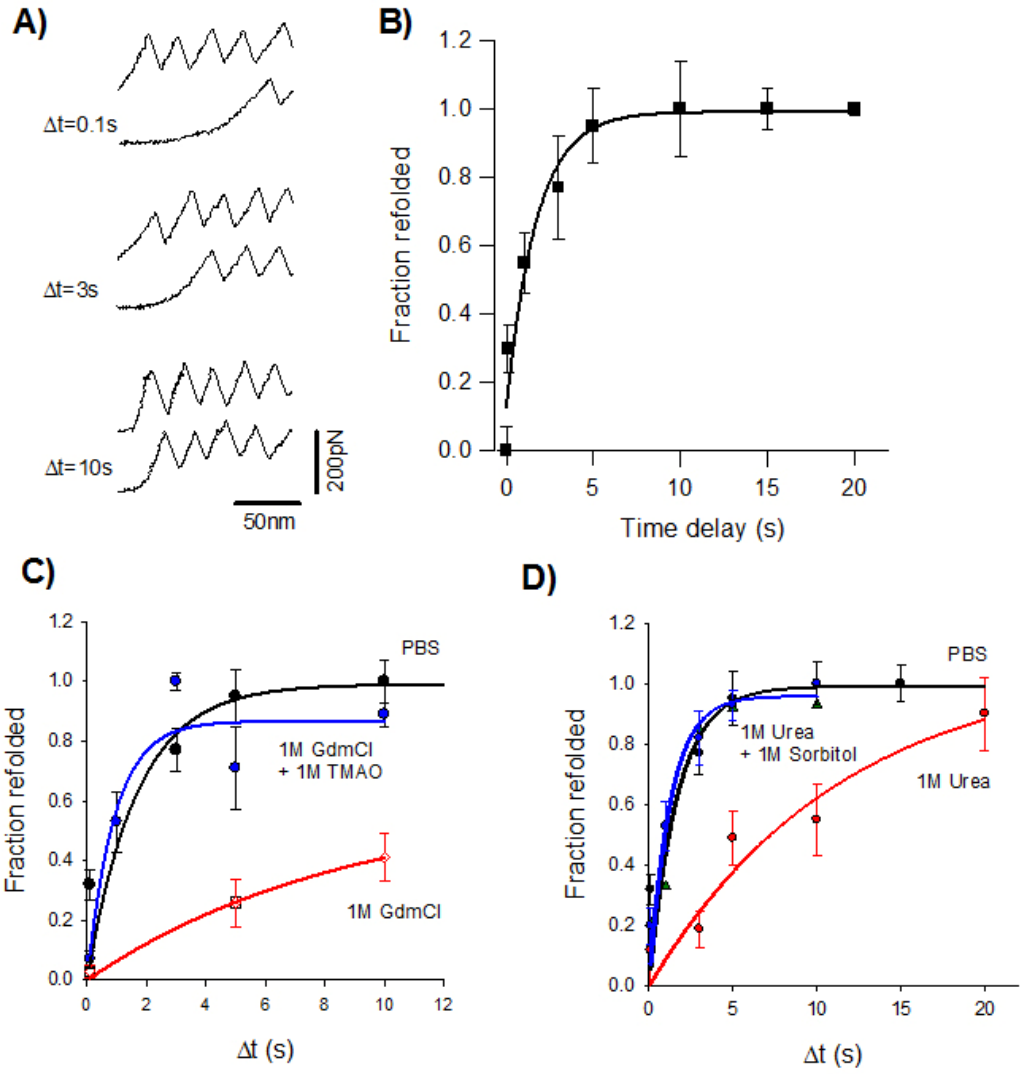

Figure 18: Effects of different combinations of denaturants and protecting osmolytes on the refolding rate of ArPKD domains. A) Measuring the refolding rate of ArPKD domains using a two-pulse stretching/relaxation protocol. Three examples obtained with time delays of 0.1, 3, and 10 s. **B)** Plot of the fraction of refolded domains as a function of the time between stretching pulses obtained in PBS. The line corresponds to a fit of the data to a single exponential with a time constant of 0.6 s^{-1}. **C)** Plot of the fraction of refolded domains vs time interval obtained in 1M GdmCl (red circles), 1M GdmCl + 1M TMAO (blue circles) and PBS (black circles). The respective time constants are: 0.04 s^{-1}, 1.2 s^{-1} and 0.6 s^{-1}. **D)** Plot of the fraction of refolded domains vs time interval obtained in 1M urea (red circles), 1M urea + 1M sorbitol (blue circles) and PBS (black circles). The respective time constants are: 0.1 s^{-1}, 0.51 s^{-1} and 0.6 s^{-1}.

In the presence of denaturants such as 1 M GdmCl and 1 M urea, the refolding rates were greatly slowed down by about 15 and 5 fold (0.04 s^{-1} and 0.1 s^{-1}, respectively; red curves in **Figure 18C, D**). I found that this slowdown of the refolding rate can be counteracted by protecting osmolytes. In the presence of a 1:1 mixture of GdmCl + TMAO or urea + sorbitol the measured refolding rates were 1.2 s^{-1} (1M GdmCl + 1M TMAO) and 0.51 s^{-1} (1M urea + 1M sorbitol), respectively (blue curves in **Figure 18C, D)**. Our results demonstrate that the refolding rate of PKD domains can be modulated by interplay of destabilizing and protecting osmolytes. This suggests that naturally occurring osmolytes may affect the elastic properties of PC1's ectodomain and thus change its mechanical function in different regions of the kidney.

4.4 DISCUSSION

4.4.1 Mechanism of action of denaturants and osmolytes

Organic osmolytes are small molecules widely used by cells and organisms to participate in cell volume regulation. In addition, they have a dramatic effect on protein function and protein folding (e.g. Street *et al.* 2006). All known osmolytes are amino acids and derivatives, polyols and sugars, methylamines, and urea (Yancey 2001). Some of these osmolytes have been shown to have a destabilizing effect (such as urea); others are known as protecting osmolytes (such methylamines and polyols) because they counteract urea's destabilizing effect. For example, four small organic molecules, belonging to trimethylamines (betaine and glycerophosphorylcholine (GPC)) and polyols (sorbitol and inositol), have been shown to stabilize proteins (Yancey 2001).

Urea, a naturally occurring osmolyte denaturant found in the kidney has been studied extensively (Tanford 1968; Greene *et al.* 1974; Santoro *et al.* 1988; Schellman 2002). The available evidence suggests that urea denaturation likely occurs through two

possible pathways (Caballero-Herrera *et al.* 2005). Urea can act 'indirectly' by altering the water structure and orientating the distribution of water molecules and perturbing hydrophobic interactions (Bennion *et al.* 2003; Idrissi 2005; Daggett 2006) (**Figure 19)**. It can also interact 'directly' through hydrogen bonding with both the peptide backbone and exposed side chains. This results in a negative free-energy contribution which forces protein to unfold (Wu *et al.* 1999; Mountain *et al.* 2003; Auton *et al.* 2005). More recent data shows that urea-induced denaturation may occur through a combination of both 'indirect' and 'direct' actions (Beck *et al.* 2007).

Protecting osmolytes are known to increase the thermodynamic stability of folded proteins and provide protection against denaturing by urea. It has been shown that protecting osmolytes, such as TMAO, sorbitol, sarcosine, and glycerol, can stabilize the native state (Auton *et al.* 2005; Street *et al.* 2006; Garcia-Manyes *et al.* 2009); however, the molecular origin of these effects remains elusive.

One of the best studied protecting osmolytes is TMAO, an osmolyte found in elasmobranches. For example, the mechanism of action has been analyzed using molecular dynamics simulation (Bennion *et al.* 2004) and bulk denaturation experiments (Baskakov *et al.* 1998). It has been suggested that it can induce ordering of the hydration layer of a polypeptide chain (**Figure 19**), thus stabilizing the native structure. It can also prevent urea from interacting with backbone and side chain hydrogen bonds thus promoting protein folding (Bennion *et al.* 2004). Recent evidence showed that TMAO tends to act as a simple "surfactant" displacing water and urea, thus eliminating the hydrophobic perturbation (Paul *et al.* 2008).

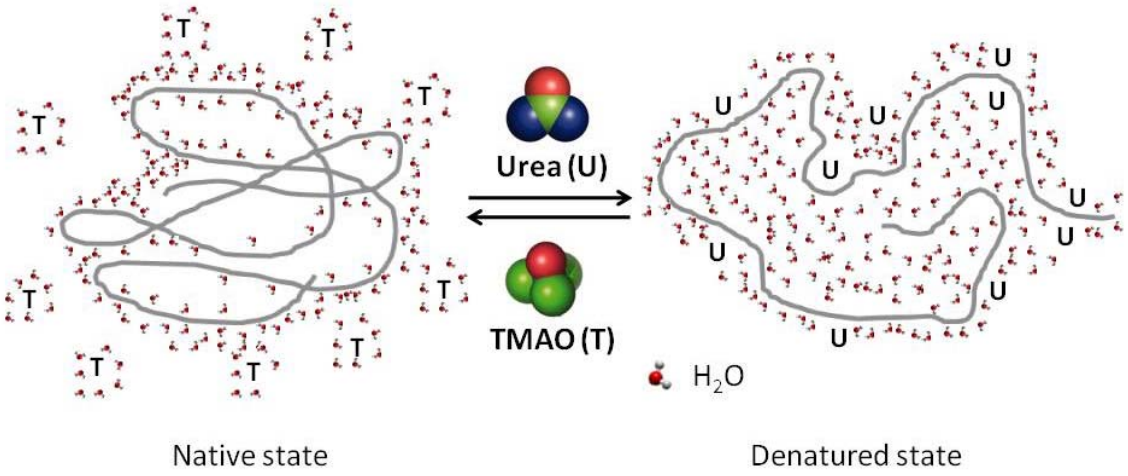

Figure 19: Model of urea and TMAO's effects on protein folding (based on published models (Yancey 2001))**.** The addition of urea promotes the protein to unfold, while TMAO promotes the protein to fold.

A simple model for the action of urea and TMAO was proposed by Wayne Bolen's group (Wang *et al.* 1997; Auton *et al.* 2005; Street *et al.* 2006). According to this model urea interacts favorably with the backbone in the unfolded polypeptide chain. This explains why urea is such an effective denaturant. On the other hand, backbone-backbone (hydrogen-bonding) interactions are greatly enhanced in the presence of TMAO, resulting in the collapse of unfolded protein and the consequent formation of secondary structure. This is why TMAO is a highly protecting osmolyte.

4.4.2 Effects of protecting osmolytes on the mechanical stability and refolding rates of PKD domains

Here I directly examined the effects of several organic protecting osmolytes on urea exposed PKD domains. I found that every osmolyte tested can counteract the destabilizing effects of urea. For example, at a ratio of 1:1, sorbitol can completely off-set the weakening effect of urea (**Figure 15**) and restore the mechanical stability of HuPKDd1 domains. This indicates that these osmolytes may play an important role in

modulating the mechanical stability of PKD domains in a harsh chemical environment, such as in kidney (Garcia-Perez *et al.* 1991).

Protecting osmolytes were also found to counteract the effect of denaturants on the refolding rate of ArPKD domains. I favor a 'direct mechanism' (Bolen *et al.* 2001; Rose *et al.* 2006) where osmolytes can interact unfavorably with highly exposed peptide backbone in the denatured state. This osmophobic effect preferentially raises the free energy of the denatured state, shifting the equilibrium in favor of the native state. A similar mechanisms has been recently described for the stabilization of the native state of ubiquitin by glycerol (Garcia-Manyes *et al.* 2009).

4.4.3 Physiological implications

Our data show that protecting osmolytes can not only strengthen the urea-weakened PKD domains, but also accelerate the refolding rate of PKD domains in urea. This underscores the important biological relevance of protecting osmolytes in physiological environment. Interestingly, sorbitol is found together with another polyol (inositol) and two trimethylamines (GPC and betaine) in the tubules of human kidney (Schmolke *et al.* 1989; Wirthensohn *et al.* 1989; Guder *et al.* 1990; Garcia-Perez *et al.* 1991; Schmolke *et al.* 1996a; Schmolke *et al.* 1996b), at an approximate high concentration of 400mM. PC1 it is constantly bearing not only mechanical forces but also denaturing stresses of urea. Other sources of forces are required to counteract urea effect in order to maintain PC1's mechanical strength and normal function *in vivo*. On the other hand, it has been reported that the distribution of sorbitol increases from the cortex to the papillary tip in mammalian kidney from rats and also in human (Schmolke *et al.* 1996; Schmolke *et al.* 1996). This is consistent with an increasing pattern of urea from proximal tubule to the collecting duct. Moreover, similar distribution pattern was observed for the

other osmolytes such as betaine and glycerophosphorylcholine (GPC) in mammalian kidney (Garcia-Perez *et al.* 1991; Schmolke *et al.* 1996b). Thus, it seems like PC1 is set into a perfectly designed well-balanced system so that it can maintain its modular structure and function as a mechanosensor under normal physiological condition.

Osmolytes such as glycerol, TMAO, GPC, sorbitol, myo-inositol and taurine are also called "chemical chaperones". For example, Welch's group reported that chemical chaperones can facilitate the maturation and function of ΔF508 CFTR, one mutant form of cystic fibrosis transmembrane conductance regulator (CFTR) with a deletion of phenylalanine at position 508. Similar effect was achieved by replacing the chemical chaperones with a small substitute molecule, *S*-nitrosoglutathione (Brown *et al.* 1996; Howard *et al.* 2003). The rationale behind this finding is that the osmolytes and equivalent substitutes enhance the hydrophobic effect of newly synthesized ΔF508 CFTR and help it to collapse an early folding intermediate that usually requires hydrophobic interactions in and around position 508. Then, this folding intermediate succeeds in going to the native state, thereby escaping the endoplasmic reticulum, maturing in the Golgi, and ultimately trafficking to the plasma membrane to become a functional ΔF508 CFTR protein. These results demonstrate the feasibility of a novel approach as a therapeutic treatment in rescuing disease-associated mutations. In ADPKD, to make chemical chaperone-based therapies clinically relevant, it requires further investigation on the possible rescuing mechanisms by which osmolytes stabilize disease-associated mutations and intensive identification of potential therapeutic candidates for the treatment of ADPKD.

Chapter 5

Conclusions and Future Experiments

5.1 Disease-associated missense mutations in PC1

In this study six missense mutations of interest (FH26L, T36C, G43S, W38R, R57L, and V59H) were screened, by using the first PKD domain of human PC1 as a model domain. It is found that these mutants altered the mechanical properties of PKD domains to different extents. In addition, the free energy of mechanical unfolding and the position of the transition state can also be affected by point mutations. They will, therefore, compromise the ability of PC1 to act as a mechanosensor.

Similar effects on thermodynamic stability of equivalent mutations were observed in the homologous PKD domain of archaebacteria. This indicates that pathogenic mutations can also affect the normal response of other PKD domains to external mechanical forces, thus it may help us to understand the molecular mechanisms underlying the physiological effects of mutations in PC1 in the future. Moreover, it may be possible to analyze naturally occurring variations in the genome sequence, predict the biophysical effect of the mutation, and estimate the likelihood of a given variation to be deleterious or benign. Results from this study also suggest that more work is required on protein function, and possibly, mutation specific therapies.

In order to obtain the detailed information how mutations alter the unfolding/refolding kinetics of PKD domains, Chevron plot-type of experiments would be an ideal approach, which is a way of representing protein folding kinetic data in the presence of varying concentrations of denaturant that disrupts the native tertiary structure of protein (e.g. Cao *et al.* 2008). In these experiments the logarithm of the observed relaxation rate is plotted as a function of the denaturant concentration.

Refolding kinetics is another important means to describe a protein's mechanical property. Based on the nature of slow refolding rate of human PKD domains (~0.04 s^{-1}), we can conclude that a mutant form would be hard to refold or may even remain unfolded. I found that the ArPKD polyprotein is suited for AFM refolding experiments. It is an ideal model protein to study the refolding kinetics of PKD domains (paper under preparation) under a number of different chemical environments. In addition this protein is much easier to express in *E. coli* than the human PKD domains. Hence, we are planning to carry out extensive mutagenesis analysis using the model protein.

5.2 EFFECTS OF NATURALLY OCCURING OSMOLYTES ON PC1 MECHANICAL FUNCTION

As predicted, the denaturants such as urea and GdmCl can alter the mechanical properties of modular proteins on two aspects, weakening their mechanical stability and slowing down their refolding rates. A steady decrease in the mechanical stability of modular domains was observed upon increasing the concentration of urea. However, different domains show different sensitivities on the increase of denaturant concentrations. HuPKDd1 was found as the most urea-sensitive domain among the ones investigated (I27, ArPKD and GB1). Fig 20A shows a plot of the thermodynamic stability of different beta-sandwich domains (measured using chemical denaturants) as a function of their sensitivity to urea concentration (measured using AFM). There is a linear relationship between the thermodynamic stability and how sensitive they are to the urea concentration. Fig 20B shows that even though they share a similar structure (beta-sandwich structure) and mechanical stability (they unfold at a similar force of ~200pN), they have different thermodynamic stability.

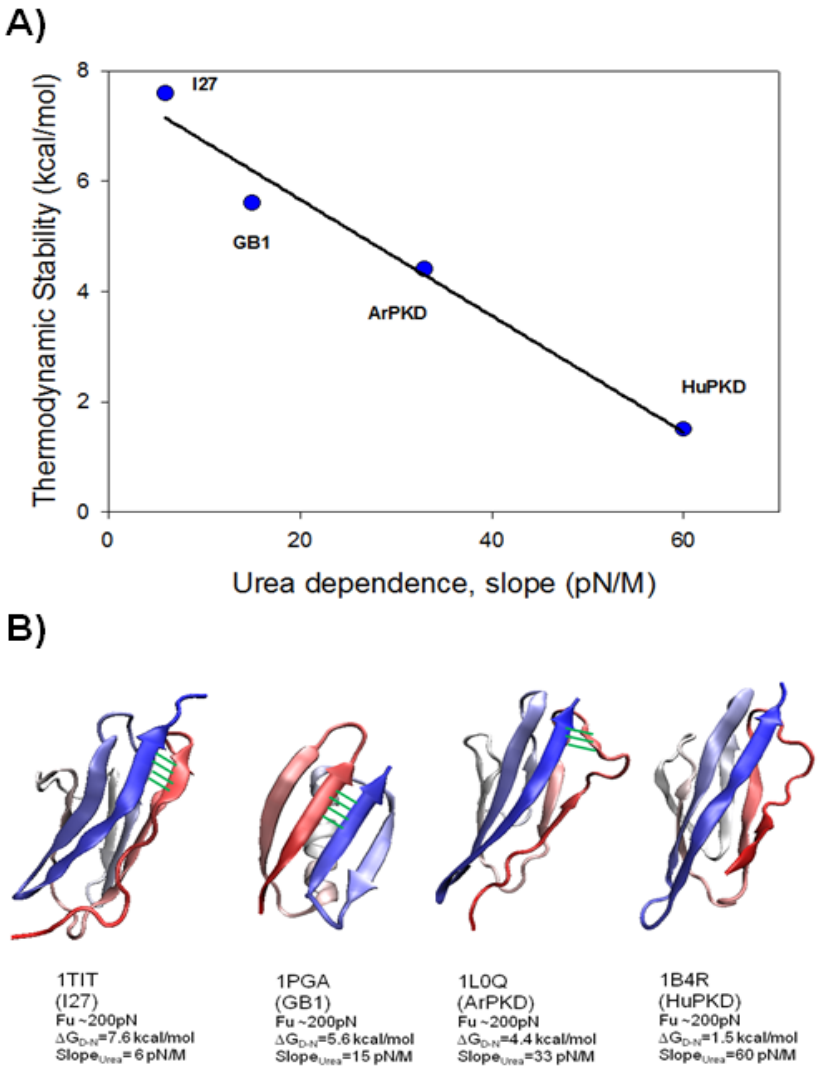

Figure 20: Comparison of the thermodynamic stability and effect of urea on mechanical stability of different beta-sandwich domains. A) Relationship of thermodynamic stability and mechanical sensitivity of different beta-sandwich fold domains to urea. **B)** Structures of the different domains. The key H-bonds that confer mechanical resistance are shown in green.

The mechanical stability is related to the mechanical topology, i.e. how the beta strands are arranged with respect the pulling force from the N- and C- terminus. The I27 is mechanically very stable because it has a relatively large number of H-bonds

connecting the force-bearing beta strands (shown as green lines in Fig. 20B). The thermodynamic stability is related to how much of the structure is exposed to the solvent (i.e. accessible surface area, ASA). The HuPKD has a low thermodynamic stability because it has a relatively large ASA compared to I27. When the domains are exposed to both chemical and mechanical forces the HuPKD is found the weakest and I27 the strongest. This is because chemical denaturants affect the global stability of the domain, whereas mechanical denaturation is vectorial and hence affects only small subset elements of their structure. The combination of both denaturating forces has synergistic effect on the overall stability of the domains.

Furthermore, we found that PKD domains unfolding through different unfolding pathways in the presence of denaturants, indicating that there are many partially folded states of these domains. This suggests that PKD domains may have several mechanical 'phenotypes' under the dynamic combination of the external mechanical force and chemical denaturation stresses.

It is very likely that osmolytes can change the unfolding kinetics of PKD domains significantly. In order to obtain more detailed information about the dynamic unfolding pathways of PKD domains and understand their unfolding kinetics in the presence of urea, a speed-dependence experiment followed by a Monte-Carlo simulation would be a helpful approach to accomplish this work (Ma *et al.* 2009). These experiments are under way.

The osmolytes in this study fall into two categories, destabilizing osmolytes (urea) and protecting osmolytes (sorbitol, TMAO and sarcosine). In this work, we were the first to systematically study how protecting osmolytes counteract the destabilizing effect of urea at single molecule level. These osmolytes were found to have a strong counteracting potential to the denaturing effect of urea, either on protein's mechanical stability or

refolding kinetics. The ratio of urea to each of protecting osmolytes that is effective in protecting PKD domains was quantified in **Figure 15**. In the physiological environment, many osmolytes were found co-existing in nephron of mammalians (Garcia-Perez *et al.* 1991). This suggests that might be more than one osmolyte counteracting the urea's denaturation effect. Is the counteracting effect of different osmolytes additive? What is the best combination in order to achieve the maximum effect? These are the interesting questions that need to be addressed in the future study in order to understand how the mechanical properties of PKD domains are modulated by the combination of urea and different protecting osmolytes.

Most of the pathogenic missense mutations destabilize PKD domains (Ma *et al.* 2009), making the protein vulnerable and favoring the denatured state. Theoretically, a small concentration of urea would cause deleterious impact on the PKD mutants. So far, it is still not clear whether there is a generally robust effect of the protecting osmolytes on different variations of PKD mutant phenotype. For a certain osmolyte, will its protecting effect be the same when it interacts with a mutant as to a wild type? Will it strengthen the PKD mutants in urea as it does to wild type? Is there a variation of stabilizing effect among different protecting osmolyte candidates on a certain mutant? Which osmolyte performs the best in terms of restoring the mechanical stability of PKD mutants? What is the optimal dosage of each osmolyte? Does an osmolyte have an optimal effect on a specific mutant? These will be interesting questions that need to be addressed in future investigations. This kind of study has the potential to provide new therapeutic approaches (*e.g.* through the use of osmolytes) for rescuing destabilized and misfolded mutant PKD domains.

References

Auton, M., and Bolen, D.W. (2005). Predicting the energetics of osmolyte-induced protein folding/unfolding. Proc Natl Acad Sci U S A *102*, 15065-15068.

Baskakov, I., and Bolen, D.W. (1998). Forcing thermodynamically unfolded proteins to fold. J Biol Chem *273*, 4831-4834.

Baskakov, I., Wang, A., and Bolen, D.W. (1998). Trimethylamine-N-oxide counteracts urea effects on rabbit muscle lactate dehydrogenase function: a test of the counteraction hypothesis. Biophys J *74*, 2666-2673.

Bateman, A., Jouet, M., MacFarlane, J., Du, J.S., Kenwrick, S., and Chothia, C. (1996). Outline structure of the human L1 cell adhesion molecule and the sites where mutations cause neurological disorders. EMBO J *15*, 6050-6059.

Beck, D.A.C., Bennion, B.J., Alonso, D.O.V., Daggett, V., Dieter, H., and Helmut, S. (2007). Simulations of Macromolecules in Protective and Denaturing Osmolytes: Properties of Mixed Solvent Systems and Their Effects on Water and Protein Structure and Dynamics. In Methods in Enzymology (Academic Press), *428*. 373-396.

Bedford, J.J., and Leader, J.P. (2007). Organic osmolytes in the developing kidney of the Australian brush-tailed possum, Trichosurus vulpecula. Comp Biochem Physiol A Mol Integr Physiol *147*, 1047-1052.

Bennion, B.J., and Daggett, V. (2003). The molecular basis for the chemical denaturation of proteins by urea. Proc Natl Acad Sci U S A *100*, 5142-5147.

Bennion, B.J., and Daggett, V. (2004). Counteraction of urea-induced protein denaturation by trimethylamine N-oxide: a chemical chaperone at atomic resolution. Proc Natl Acad Sci U S A *101*, 6433-6438.

Best, R.B., and Clarke, J. (2002a). What can atomic force microscopy tell us about protein folding? Chem Commun (Camb) *2002*, 183-192.

Best, R.B., Fowler, S.B., Toca-Herrera, J.L., and Clarke, J. (2002b). A simple method for probing the mechanical unfolding pathway of proteins in detail. Proc Natl Acad Sci U S A *99*, 12143-12148.

Best, R.B., Li, B., Steward, A., Daggett, V., and Clarke, J. (2001). Can non-mechanical proteins withstand force? Stretching barnase by atomic force microscopy and molecular dynamics simulation. Biophys J *81*, 2344-2356.

Bolen, D.W. (2001). Protein stabilization by naturally occurring osmolytes. Methods Mol Biol *168*, 17-36.

Bolen, D.W., and Baskakov, I.V. (2001). The osmophobic effect: Natural selection of a thermodynamic force in protein folding. J Mol Biol *310*, 955-963.

Boletta, A., and Germino, G.G. (2003). Role of polycystins in renal tubulogenesis. Trends Cell Biol *13*, 484-492.

Brown, C.R., Hong-Brown, L.Q., Biwersi, J., Verkman, A.S., and Welch, W.J. (1996). Chemical chaperones correct the mutant phenotype of the delta F508 cystic

fibrosis transmembrane conductance regulator protein. Cell Stress Chaperones *1*, 117-125.

Brucale, M., Sandal, M., Di Maio, S., Rampioni, A., Tessari, I., Tosatto, L., Bisaglia, M., Bubacco, L., and Samori, B. (2009). Pathogenic mutations shift the equilibria of alpha-synuclein single molecules towards structured conformers. Chembiochem *10*, 176-183.

Bullard, B., Linke, W.A., and Leonard, K. (2002). Varieties of elastic protein in invertebrate muscles. J Muscle Res Cell Motil *23*, 435-447.

Burtey, S., Lossi, A.M., Bayle, J., Berland, Y., and Fontes, M. (2002). Mutation screening of the PKD1 transcript by RT-PCR. J Med Genet *39*, 422-429.

Bustamante, C., Macosko, J.C., and Wuite, G.J. (2000). Grabbing the cat by the tail: manipulating molecules one by one. Nat Rev Mol Cell Biol *1*, 130-136.

Bustamante, C., Marko, J.F., Siggia, E.D., and Smith, S. (1994). Entropic elasticity of lambda-phage DNA. Science *265*, 1599-1600.

Bycroft, M., Bateman, A., Clarke, J., Hamill, S.J., Sandford, R., Thomas, R.L., and Chothia, C. (1999). The structure of a PKD domain from polycystin-1: implications for polycystic kidney disease. EMBO J *18*, 297-305.

Caballero-Herrera, A., Nordstrand, K., Berndt, K.D., and Nilsson, L. (2005). Effect of urea on peptide conformation in water: molecular dynamics and experimental characterization. Biophys J *89*, 842-857.

Cao, Y., and Li, H. (2008). Engineered elastomeric proteins with dual elasticity can be controlled by a molecular regulator. Nat Nanotechnol *3*, 512-516.

Carrion-Vazquez, M., Oberhauser, A.F., Fisher, T.E., Marszalek, P.E., Li, H., and Fernandez, J.M. (2000). Mechanical design of proteins studied by single-molecule force spectroscopy and protein engineering. Prog Biophys Mol Biol *74*, 63-91.

Carrion-Vazquez, M., Oberhauser, A.F., Fowler, S.B., Marszalek, P.E., Broedel, S.E., Clarke, J., and Fernandez, J.M. (1999). Mechanical and chemical unfolding of a single protein: a comparison. Proc Natl Acad Sci U S A *96*, 3694-3699.

Colonna, G., Alexander, S.S., Jr., Yamada, K.M., Pastan, I., and Edelhoch, H. (1978). The stability of cell surface protein to surfactants and denaturants. J Biol Chem *253*, 7787-7790.

Daggett, V. (2006). Protein folding-simulation. Chem Rev *106*, 1898-1916.

Dietz, H., Bertz, M., Schlierf, M., Berkemeier, F., Bornschlogl, T., Junker, J.P., and Rief, M. (2006). Cysteine engineering of polyproteins for single-molecule force spectroscopy. Nat Protoc *1*, 80-84.

Fisher, T.E., Carrion-Vazquez, M., Oberhauser, A.F., Li, H., Marszalek, P.E., and Fernandez, J.M. (2000). Single molecular force spectroscopy of modular proteins in the nervous system. Neuron *27*, 435-446.

Fisher, T.E., Marszalek, P.E., Oberhauser, A.F., Carrion-Vazquez, M., and Fernandez, J.M. (1999a). The micro-mechanics of single molecules studied with atomic force microscopy. J Physiol *520 Pt 1*, 5-14.

Fisher, T.E., Oberhauser, A.F., Carrion-Vazquez, M., Marszalek, P.E., and Fernandez, J.M. (1999b). The study of protein mechanics with the atomic force microscope. Trends Biochem Sci *24*, 379-384.

Florin, E.L., Rief, M., Lehmann, H., Ludwig, M., Dornmair, C., Moy, V.T., and Gaub, H.E. (1995). Sensing Specific Molecular-Interactions with the Atomic-Force Microscope. Biosensors & Bioelectronics *10*, 895-901.

Forman, J.R., Qamar, S., Paci, E., Sandford, R.N., and Clarke, J. (2005). The remarkable mechanical strength of polycystin-1 supports a direct role in mechanotransduction. J Mol Biol *349*, 861-871.

Forman, J.R., Yew, Z.T., Qamar, S., Sandford, R.N., Paci, E., and Clarke, J. (2009). Non-native interactions are critical for mechanical strength in PKD domains. Structure *17*, 1582-1590.

Gabow, P.A. (1990). Autosomal dominant polycystic kidney disease--more than a renal disease. Am J Kidney Dis *16*, 403-413.

Garcia-Manyes, S., Dougan, L., Badilla, C.L., Brujic, J., and Fernandez, J.M. (2009). Direct observation of an ensemble of stable collapsed states in the mechanical folding of ubiquitin. Proc Natl Acad Sci U S A *106*, 10534-10539.

Garcia-Perez, A., and Burg, M.B. (1991). Renal medullary organic osmolytes. Physiol Rev *71*, 1081-1115.

Garcia, T.I., Oberhauser, A.F., and Braun, W. (2009). Mechanical stability and differentially conserved physical-chemical properties of titin Ig-domains. Proteins *75*, 706-718.

Geng, L., Segal, Y., Pavlova, A., Barros, E.J., Lohning, C., Lu, W., Nigam, S.K., Frischauf, A.M., Reeders, S.T., and Zhou, J. (1997). Distribution and developmentally regulated expression of murine polycystin. Am J Physiol *272*, 451-459.

Geng, L., Segal, Y., Peissel, B., Deng, N., Pei, Y., Carone, F., Rennke, H.G., Glucksmann-Kuis, A.M., Schneider, M.C., Ericsson, M., and Zhou, J. (1996). Identification and localization of polycystin, the PKD1 gene product. J Clin Invest *98*, 2674-2682.

Goyton, A.C., and Hall, J.E. (1997). Human Physiology and Mechanisms of Disease, Sixth edition edn (W.B. Saunders Co.).

Greene, R.F., Jr., and Pace, C.N. (1974). Urea and guanidine hydrochloride denaturation of ribonuclease, lysozyme, alpha-chymotrypsin, and beta-lactoglobulin. J Biol Chem *249*, 5388-5393.

Guder, W.G., Beck, F.X., and Schmolke, M. (1990). Regulation and localization of organic osmolytes in mammalian kidney. Klin Wochenschr *68*, 1091-1095.

Hanaoka, K., Qian, F., Boletta, A., Bhunia, A.K., Piontek, K., Tsiokas, L., Sukhatme, V.P., Guggino, W.B., and Germino, G.G. (2000). Co-assembly of polycystin-1 and -2 produces unique cation-permeable currents. Nature *408*, 990-994.

Howard, M., Fischer, H., Roux, J., Santos, B.C., Gullans, S.R., Yancey, P.H., and Welch, W.J. (2003). Mammalian osmolytes and S-nitrosoglutathione promote Delta F508

cystic fibrosis transmembrane conductance regulator (CFTR) protein maturation and function. J Biol Chem *278*, 35159-35167.

Hughes, J., Ward, C.J., Peral, B., Aspinwall, R., Clark, K., San Millan, J.L., Gamble, V., and Harris, P.C. (1995). The polycystic kidney disease 1 (PKD1) gene encodes a novel protein with multiple cell recognition domains. Nat Genet *10*, 151-160.

Ibraghimov-Beskrovnaya, O., Dackowski, W.R., Foggensteiner, L., Coleman, N., Thiru, S., Petry, L.R., Burn, T.C., Connors, T.D., Van Raay, T., Bradley, J., Qian F., Onuchic, L.F., Watnick, T.J., Piontek, K., Hakim, R.M., Landes, G.M., Germino, G.G., Sandford, R., and Klinger K.W. (1997). Polycystin: in vitro synthesis, in vivo tissue expression, and subcellular localization identifies a large membrane-associated protein. Proc Natl Acad Sci U S A *94*, 6397-6402.

Idrissi, A. (2005). Molecular structure and dynamics of liquids: aqueous urea solutions. Spectrochim Acta A Mol Biomol Spectrosc *61*, 1-17.

Ignatova, Z., and Gierasch, L.M. (2006). Inhibition of protein aggregation in vitro and in vivo by a natural osmoprotectant. Proc Natl Acad Sci U S A *103*, 13357-13361.

Ikeda, M., and Guggino, W.B. (2002). Do polycystins function as cation channels? Curr Opin Nephrol Hypertens *11*, 539-545.

Itoh, H., Takahashi, A., Adachi, K., Noji, H., Yasuda, R., Yoshida, M., and Kinosita, K. (2004). Mechanically driven ATP synthesis by F1-ATPase. Nature *427*, 465-468.

Jaalouk, D.E., and Lammerding, J. (2009). Mechanotransduction gone awry. Nat Rev Mol Cell Biol *10*, 63-73.

Jing, H., Takagi, J., Liu, J.H., Lindgren, S., Zhang, R.G., Joachimiak, A., Wang, J.H., and Springer, T.A. (2002). Archaeal surface layer proteins contain beta propeller, PKD, and beta helix domains and are related to metazoan cell surface proteins. Structure *10*, 1453-1464.

Kumar, R., Baskakov, I.V., Srinivasan, G., Bolen, D.W., Lee, J.C., and Thompson, E.B. (1999). Interdomain signaling in a two-domain fragment of the human glucocorticoid receptor. J Biol Chem *274*, 24737-24741.

Li, H., Carrion-Vazquez, M., Oberhauser, A.F., Marszalek, P.E., and Fernandez, J.M. (2000). Point mutations alter the mechanical stability of immunoglobulin modules. Nat Struct Biol *7*, 1117-1120.

Li, H., Linke, W.A., Oberhauser, A.F., Carrion-Vazquez, M., Kerkvliet, J.G., Lu, H., Marszalek, P.E., and Fernandez, J.M. (2002). Reverse engineering of the giant muscle protein titin. Nature *418*, 998-1002.

Li, L., Huang, H.H., Badilla, C.L., and Fernandez, J.M. (2005). Mechanical unfolding intermediates observed by single-molecule force spectroscopy in a fibronectin type III module. J Mol Biol *345*, 817-826.

Linke, W.A., and Grutzner, A. (2008). Pulling single molecules of titin by AFM--recent advances and physiological implications. Pflugers Arch *456*, 101-115.

Loo, T.W., and Clarke, D.M. (2007). Chemical and pharmacological chaperones as new therapeutic agents. Expert Rev Mol Med *9*, 1-18.

Ma, L., Xu, M., Forman, J.R., Clarke, J., and Oberhauser, A.F. (2009). Naturally occurring mutations alter the stability of polycystin-1 polycystic kidney disease (PKD) domains. J Biol Chem *284*, 32942-32949.

Marko, J.F., and Siggia, E.D. (1995). Statistical-Mechanics of Supercoiled DNA. Phys Rev E *52*, 2912-2938.

Mathura, V.S., Schein, C.H., and Braun, W. (2003). Identifying property based sequence motifs in protein families and superfamilies: application to DNase-1 related endonucleases. Bioinformatics *19*, 1381-1390.

Mehta, A.D., Rief, M., and Spudich, J.A. (1999). Biomechanics, one molecule at a time. J Biol Chem *274*, 14517-14520.

Miller, E., Garcia, T., Hultgren, S., and Oberhauser, A.F. (2006). The mechanical properties of E. coli type 1 pili measured by atomic force microscopy techniques. Biophys J *91*, 3848-3856.

Mochizuki, T., Wu, G., Hayashi, T., Xenophontos, S.L., Veldhuisen, B., Saris, J.J., Reynolds, D.M., Cai, Y., Gabow, P.A., Pierides, A., Kimberling, W.J., Breuning, M.H., Deltas, C.C., Peters, D.J., and Somlo, S. (1996). PKD2, a gene for polycystic kidney disease that encodes an integral membrane protein. Science *272*, 1339-1342.

Mountain, R.D., and Thirumalai, D. (2003). Molecular dynamics simulations of end-to-end contact formation in hydrocarbon chains in water and aqueous urea solution. J Am Chem Soc *125*, 1950-1957.

Moy, G.W., Mendoza, L.M., Schulz, J.R., Swanson, W.J., Glabe, C.G., and Vacquier, V.D. (1996). The sea urchin sperm receptor for egg jelly is a modular protein with extensive homology to the human polycystic kidney disease protein, PKD1. J Cell Biol *133*, 809-817.

Muller, D.J., Krieg, M., Alsteens, D., and Dufrene, Y.F. (2009). New frontiers in atomic force microscopy: analyzing interactions from single-molecules to cells. Curr Opin Biotechnol.

Nauli, S.M., Alenghat, F.J., Luo, Y., Williams, E., Vassilev, P., Li, X., Elia, A.E., Lu, W., Brown, E.M., Quinn, S.J., Ingber, D.E., and Zhou, J. (2003). Polycystins 1 and 2 mediate mechanosensation in the primary cilium of kidney cells. Nat Genet *33*, 129-137.

Nauli, S.M., and Zhou, J. (2004). Polycystins and mechanosensation in renal and nodal cilia. Bioessays *26*, 844-856.

Oberhauser, A.F., Badilla-Fernandez, C., Carrion-Vazquez, M., and Fernandez, J.M. (2002). The mechanical hierarchies of fibronectin observed with single-molecule AFM. J Mol Biol *319*, 433-447.

Oberhauser, A.F., and Carrion-Vazquez, M. (2008). Mechanical biochemistry of proteins one molecule at a time. J Biol Chem *283*, 6617-6621.

Oberhauser, A.F., Hansma, P.K., Carrion-Vazquez, M., and Fernandez, J.M. (2001). Stepwise unfolding of titin under force-clamp atomic force microscopy. Proc Natl Acad Sci U S A *98*, 468-472.

Oberhauser, A.F., Marszalek, P.E., Erickson, H.P., and Fernandez, J.M. (1998). The molecular elasticity of the extracellular matrix protein tenascin. Nature *393*, 181-185.

Pace, C.N. (1975). The stability of globular proteins. CRC Crit Rev Biochem *3*, 1-43.

Pace, C.N. (1986). Determination and analysis of urea and guanidine hydrochloride denaturation curves. Methods Enzymol *131*, 266-280.

Palsson, R., Sharma, C.P., Kim, K., McLaughlin, M., Brown, D., and Arnaout, M.A. (1996). Characterization and cell distribution of polycystin, the product of autosomal dominant polycystic kidney disease gene 1. Mol Med *2*, 702-711.

Paul, S., and Patey, G.N. (2008). Hydrophobic interactions in urea-trimethylamine-N-oxide solutions. J Phys Chem B *112*, 11106-11111.

Phakdeekitcharoen, B., Watnick, T.J., Ahn, C., Whang, D.Y., Burkhart, B., and Germino, G.G. (2000). Thirteen novel mutations of the replicated region of PKD1 in an Asian population. Kidney Int *58*, 1400-1412.

Pirson, Y., Chauveau, D., and Grunfeld, J.P. (1998). Autosomal dominant polycystic renal disease. (Oxford, UK, Oxford Univerisity Press).

Praetorius, H.A., and Spring, K.R. (2001). Bending the MDCK cell primary cilium increases intracellular calcium. J Membr Biol *184*, 71-79.

Praetorius, H.A., and Spring, K.R. (2003). Removal of the MDCK cell primary cilium abolishes flow sensing. J Membr Biol *191*, 69-76.

Qian, F., Germino, F.J., Cai, Y., Zhang, X., Somlo, S., and Germino, G.G. (1997). PKD1 interacts with PKD2 through a probable coiled-coil domain. Nat Genet *16*, 179-183.

Qian, F., Wei, W., Germino, G., and Oberhauser, A. (2005). The nanomechanics of polycystin-1 extracellular region. J Biol Chem *280*, 40723-40730.

Ramachandran, G.N., Ramakrishnan, C., and Sasisekharan, V. (1963). Stereochemistry of polypeptide chain configurations. J Mol Biol *7*, 95-99.

Randles, L.G., Lappalainen, I., Fowler, S.B., Moore, B., Hamill, S.J., and Clarke, J. (2006). Using model proteins to quantify the effects of pathogenic mutations in Ig-like proteins. J Biol Chem *281*, 24216-24226.

Ratnaparkhi, G.S., and Varadarajan, R. (2001). Osmolytes stabilize ribonuclease S by stabilizing its fragments S protein and S peptide to compact folding-competent states. J Biol Chem *276*, 28789-28798.

Rief, M., Gautel, M., Oesterhelt, F., Fernandez, J.M., and Gaub, H.E. (1997). Reversible unfolding of individual titin immunoglobulin domains by AFM. Science *276*, 1109-1112.

Rief, M., and Grubmuller, H. (2002). Force spectroscopy of single biomolecules. Chemphyschem *3*, 255-261.

Rose, G.D., Fleming, P.J., Banavar, J.R., and Maritan, A. (2006). A backbone-based theory of protein folding. Proc Natl Acad Sci U S A *103*, 16623-16633.

Rossetti, S., Chauveau, D., Kubly, V., Slezak, J.M., Saggar-Malik, A.K., Pei, Y., Ong, A.C., Stewart, F., Watson, M.L., Bergstralh, E.J., Winearls, C.G., Torres, V.E., and Harris, P.C. (2003). Association of mutation position in polycystic kidney

disease 1 (PKD1) gene and development of a vascular phenotype. Lancet *361*, 2196-2201.

Rossetti, S., Chauveau, D., Walker, D., Saggar-Malik, A., Winearls, C.G., Torres, V.E., and Harris, P.C. (2002). A complete mutation screen of the ADPKD genes by DHPLC. Kidney Int *61*, 1588-1599.

Rossetti, S., Consugar, M.B., Chapman, A.B., Torres, V.E., Guay-Woodford, L.M., Grantham, J.J., Bennett, W.M., Meyers, C.M., Walker, D.L., Bae, K., Zhang, Q.J., Thompson, P.A., Miller, J.P., and Harris, P.C. (2007). Comprehensive molecular diagnostics in autosomal dominant polycystic kidney disease. J Am Soc Nephrol *18*, 2143-2160.

Rossetti, S., Strmecki, L., Gamble, V., Burton, S., Sneddon, V., Peral, B., Roy, S., Bakkaloglu, A., Komel, R., Winearls, C.G., and Harris, P.C. (2001). Mutation analysis of the entire PKD1 gene: genetic and diagnostic implications. Am J Hum Genet *68*, 46-63.

Rounsevell, R.W., Steward, A., and Clarke, J. (2005). Biophysical investigations of engineered polyproteins: implications for force data. Biophys J *88*, 2022-2029.

Sakaki, N., Shimo-Kon, R., Adachi, K., Itoh, H., Furuike, S., Muneyuki, E., Yoshida, M., and Kinosita, K., Jr. (2005). One rotary mechanism for F1-ATPase over ATP concentrations from millimolar down to nanomolar. Biophys J *88*, 2047-2056.

Samori, B. (2000). Stretching single molecules along unbinding and unfolding pathways with the scanning force microscope. Chemistry *6*, 4249-4255.

Sandford, R., Sgotto, B., Aparicio, S., Brenner, S., Vaudin, M., Wilson, R.K., Chissoe, S., Pepin, K., Bateman, A., Chothia, C., Hughes, J., and Harris, P. (1997). Comparative analysis of the polycystic kidney disease 1 (PKD1) gene reveals an integral membrane glycoprotein with multiple evolutionary conserved domains. Hum Mol Genet *6*, 1483-1489.

Santoro, M.M., and Bolen, D.W. (1988). Unfolding free energy changes determined by the linear extrapolation method. 1. Unfolding of phenylmethanesulfonyl alpha-chymotrypsin using different denaturants. Biochemistry *27*, 8063-8068.

Schellman, J.A. (2002). Fifty years of solvent denaturation. Biophys Chem *96*, 91-101.

Schmolke, M., Bornemann, A., and Guder, W.G. (1996a). Site-specific regulation of organic osmolytes along the rat nephron. Am J Physiol-Renal *40*, 645-652.

Schmolke, M., and Guder, W.G. (1989). Metabolic regulation of organic osmolytes in tubules from rat renal inner and outer medulla. Ren Physiol Biochem *12*, 347-358.

Schmolke, M., Schilling, A., Keiditsch, E., and Guder, W.G. (1996b). Intrarenal distribution of organic osmolytes in human kidney. Eur J Clin Chem Clin *34*, 499-501.

Sharif-Naeini, R., Folgering, J.H., Bichet, D., Duprat, F., Lauritzen, I., Arhatte, M., Jodar, M., Dedman, A., Chatelain, F.C., Schulte, U., Retailleau, K., Loufrani, L., Patel A., Sachs, F., Delmas, P., Peters, D.J.M., and Honoré, E. (2009). Polycystin-1 and -2 dosage regulates pressure sensing. Cell *139*, 587-596.

Steward, A., Toca-Herrera, J.L., and Clarke, J. (2002). Versatile cloning system for construction of multimeric proteins for use in atomic force microscopy. Protein Sci *11*, 2179-2183.

Street, T.O., Bolen, D.W., and Rose, G.D. (2006). A molecular mechanism for osmolyte-induced protein stability. Proc Natl Acad Sci U S A *103*, 13997-14002.

Street, T.O., Krukenberg, K.A., Rosgen, J., Bolen, D.W., and Agard, D.A. (2009). Osmolyte-induced conformational changes in the Hsp90 molecular chaperone. Protein Sci *19*, 57-65.

Sundberg, M., Rosengren, J.P., Bunk, R., Lindahl, J., Nicholls, I.A., Tagerud, S., Omling, P., Montelius, L., and Mansson, A. (2003). Silanized surfaces for in vitro studies of actomyosin function and nanotechnology applications. Analytical Biochem *323*, 127-138.

Sutters, M. (2006). The pathogenesis of autosomal dominant polycystic kidney disease. Nephron Exp Nephrol *103*, 149-155.

Tanford, C. (1968). Protein denaturation. Adv Protein Chem *23*, 121-282.

Thomas, R., McConnell, R., Whittacker, J., Kirkpatrick, P., Bradley, J., and Sandford, R. (1999). Identification of mutations in the repeated part of the autosomal dominant polycystic kidney disease type 1 gene, PKD1, by long-range PCR. Am J Hum Genet *65*, 39-49.

Tsiokas, L., Kim, S., and Ong, E.C. (2007). Cell biology of polycystin-2. Cell Signal *19*, 444-453.

Venkatesu, P., Lee, M.J., and Lin, H.M. (2009). Osmolyte counteracts urea-induced denaturation of alpha-chymotrypsin. J Phys Chem B *113*, 5327-5338.

Wang, A., and Bolen, D.W. (1997). A naturally occurring protective system in urea-rich cells: mechanism of osmolyte protection of proteins against urea denaturation. Biochemistry *36*, 9101-9108.

Wirthensohn, G., Lefrank, S., Schmolke, M., and Guder, W.G. (1989). Regulation of organic osmolyte concentrations in tubules from rat renal inner medulla. Am J Physiol *256*, F128-135.

Wu, J.W., and Wang, Z.X. (1999). New evidence for the denaturant binding model. Protein Sci *8*, 2090-2097.

Yancey, P.H. (2001). Water stress, osmolytes and proteins. American Zoologist *41*, 699-709.

Yancey, P.H., Clark, M.E., Hand, S.C., Bowlus, R.D., and Somero, G.N. (1982). Living with water stress: evolution of osmolyte systems. Science *217*, 1214-1222.

Zou, Q., Bennion, B.J., Daggett, V., and Murphy, K.P. (2002). The molecular mechanism of stabilization of proteins by TMAO and its ability to counteract the effects of urea. J Am Chem Soc *124*, 1192-1202.

Vita

NAME: LIANG MA

ADDRESS: 6911 Weiss Dr., Galveston, TX, 77551

BIOGRAPHICAL: April 6, 1978, Liaoyang, Liaoning, P.R.China.
Father: Jiquan Ma
Mother: Yufen Liang

EDUCATION: July, 2000. B.A. (Marine Biology),
Xiamen University, Xiamen, Fujian, P.R.China

May, 2006. M.S. (Fish Genetics),
Texas A&M University, College Station, Texas, USA

Present, Ph.D. Candidate
(Cell Physiology and Molecular Biophysics),
University of Texas Medical Branch, Galveston, Texas, USA

PROFESSIONAL AND TEACHING EXPERIENCE:

10/1998-07/2002: **Research Assistant**
Marine Biochemistry and Ecology Laboratory
Department of Oceanography
Xiamen University, Xiamen, Fujian, P.R. China

02/2001-07/2001: **Teaching Assistant (in Ichthyology)**
Department of Oceanography
Xiamen University, Xiamen, Fujian, P.R. China

09/2002-05/2003: **Teaching Assistant (in Genetics)**
College of Agriculture and Life Sciences
Texas A&M University, College Station, Texas, USA

06/2003-08/2003 **Research Assistant**
01/2004-08/2004 Fish Genetics Laboratory
01/2005-05/2005: College of Agriculture and Life Sciences
Texas A&M University, College Station, Texas, USA

09/2003-12/2003 **Teaching Assistant (in Ichthyology)**
09/2004-12/2004: College of Agriculture and Life Sciences
Texas A&M University, College Station, Texas, USA

06/2005-09/2006: **Research Associate I**
Department of Neuroscience and Cell Biology

The University of Texas Medical Branch, Galveston, Texas, USA

09/2006-08/2010: **Research Assistant**
Department of Neuroscience and Cell Biology
The University of Texas Medical Branch, Galveston, Texas, USA

HONORS:

- *Dennis Bowman Memorial Scholarship Award*, UTMB, 2009
- *Mason Guest Scholarship Award*, UTMB, 2009
- *Margaret Saunders Travel Scholarship Award*, UTMB, 2008
- *Mason Guest Scholarship Award*, UTMB, 2008
- Best Performance Award in Graduate Student Poster Presentation (13th Annual Structural Biology Symposiums), 2008
- Best Graduate Student Podium Presentation Award (5th Annual Dept. Research Retreat), 2008
- Best Graduate Student Poster Presentation Award (4th Annual Dept. Research Retreat), 2007

PUBLICATIONS

A. ARTICLES IN PEER-REVIEWED JOURNALS :

- ***Ma, L.***, Xu, M., Forman, J.R., Clarke, J. and Oberhauser, A.F. Naturally occurring Mutations alter the Stability of Polycystin-1 PKD Domains. The Journal of Biological Chemistry, 284 (47): 32942-32949, 2009.
- ***Ma, L.***, Xu, M. and Oberhauser, A.F. Single-molecule Force Spectroscopy of Polycystic Kidney Disease Proteins. Humana Press Book Chapter, May, 2009.
- Futton, K., ***Ma, L.***, Sutton, R.B. and Oberhauser, A.F. The C2 domains of human synaptotagmin 1 have distinct mechanical properties. Biophysical Journal 96 (3): 1083-1090, 2009.
- ***Ma, L.***, Saillant, E., Gatlin III, D.M. and Gold, J.R. Estimates of heritability of larval and early juvenile growth traits in red drum (*Sciaenops ocellatus*). Journal of Applied Aquaculture 20 (2): 134-147, 2008.
- Gold, J.R., ***Ma, L.***, Saillant, E., Silva, P.S. and Vega, R.R.. Genetic effective size in populations of hatchery-rased red drum released for stock enhancement. Transaction of the American Fisheries Society 137: 1327-1334, 2008.
- Saillant, E., Wang, X., ***Ma, L.***, Gatlin III, D.M., Vega, R.R. and Gold, J.R.. Heritability of tolerance to acute cold stress in red drum, *Sciaenops ocellatus*. Aquaculture Research. (published online: May 22, 2008)
- ***Ma, L.***, Saillant, E., Gatlin III, D.M. and Gold, J.R.

Heritability of cold tolerance in red drum. North America Journal of Aquaculture 69 (4): 381-387, 2007.

- Saillant, E., ***Ma, L.***, Wang, X., Gatlin III, D.M. and Gold, J.R. Heritability of juvenile growth traits in red drum (*Sciaenops ocellatus* L.). Aquaculture Research 38: 781-788, 2007.
- Karlsson, S., ***Ma, L.***, Saillant, E. and Gold, J.R. Tests of Mendelian segregation and linkage-group relationships among 31 microsatellite loci in red drum, *Sciaenops ocellatus*. Aquaculture International 15 (5): 383-391, 2007.
- Clark, T. B., ***Ma, L.***, Saillant, E. and Gold, J.R. Microsatellite DNA markers for population-genetic studies of Atlantic bluefin tuna (*Thunnus thynnus thynnus*) and other species of genus *Thunnus*. Molecular Ecology Notes 4: 70-73, 2004.
- ***Ma, L.***, Wang, J., Chen, W., Su, Y., Ding, S., Wang, D. and You, Y. The study on the fetation of two drumfishes crossbreeding filial generation Ⅰ. Journal of Xiamen University (Natural Science) 41: 378-382, 2002.
- Wang, J., Wang, D., You, Y., Su, Y., Ding, S., ***Ma, L.*** and Chen, W. Preliminary study on induction of triploidy in *Pseudosciaena crocea*. Journal of Xiamen University (Natural Science) 40: 927-930, 2001.
- Wang, J., Yan, Q., Su, Y., ***Ma, L.*** and Sao, X. Study on indirect ELISA method for detecting *Vibrio parahaemolyticus* in cultured *Pseudosciaena crocea*. Journal of Oceanography in Taiwan Strait 20: 346-351, 2001.
- Ding, S., Wang, J., Su, Y., Quan, C., Zhang, W., Guo, F., and ***Ma, L.*** Allozyme analysis of genetic diversity in culture *Plectorhinchus cinctus*. Journal of Oceanography in Taiwan Strait 20: 224-228, 2001.
- Zhang, Z., Su, Y., Wang, J., Yan, Q. and ***Ma, L.*** Studies on the Pathogen of *Penaeus monodon Vibrio fluvialis* Type Ⅰ. ACTA Scientiarum Naturalium Universitatis Sunyatsent 39: 208-213, 2000.

B. ABSTRACTS (POSTERS & PRESENTATIONS):

- ***Ma, L.***, Xu, M. and Oberhauser, A.F. Nanoscale analysis of the effect of pathogenic mutations on Polycystin-1. 2010 ASME International 1st Global Congress on Nano Engineering for Medicine & Biology (NEMB) 2010 Advancing Health Care Through Nano-Engineering & Computations. February, 2010

- Xu, M., ***Ma, L.*** and Oberhauser, A.F. How do osmolytes affect the stability of polycystin-1 PKD domains? Biophysical Society 54th Annual Meeting, San Francisco, CA, February, 2010
- ***Ma, L.***, Xu, M. and Oberhauser, A.F. How do osmolytes affect the stability of polycystin-1 PKD domains? Biomolecular Interactions & Methods, January, 2010
- ***Ma, L.***, Xu, M. and Oberhauser, A.F. How do osmolytes affect the stability of polycystin-1 PKD domains? The 6th Annual Research Retreat 2009. University of Texas Medical Branch, Galveston, TX, October, 2009
- Xu, M., ***Ma, L.*** and Oberhauser, A.F. Mechanical function and Biophysical Properties of the REJ region of Polycystin-1. The 14th Annual Structural Biology Symposium 2009. University of Texas Medical Branch, Galveston, TX, May, 2009
- ***Ma, L.***, Xu, M. and Oberhauser, A.F. Pathogenic Mutations alter the Mechanical Stability of Polycystin-1 Immunoglobulin PKD Domains. The 14th Annual Structural Biology Symposium 2009. University of Texas Medical Branch, Galveston, TX, May, 2009
- Xu, M., ***Ma, L.*** and Oberhauser, A.F. Mechanical function and Biophysical Properties of the REJ region of Polycystin-1. Biophysical Society 53rd Annual Meeting, Boston, MA, February, 2009
- ***Ma, L.***, Xu, M. and Oberhauser, A.F. Pathogenic Mutations alter the Mechanical Stability of Polycystin-1 Immunoglobulin PKD Domains. The Biophysical Society 53rd Annual Meeting. Boston, MA, February, 2009
- Xu, M., Delgado, E., Odunuga, O., ***Ma, L.*** and Oberhauser, A.F. The Nanomechanics of the REJ Region of Polycystin-1. The 5th Annual Research Retreat 2008. University of Texas Medical Branch, Galveston, TX, July, 2008
- ***Ma, L.***, Xu, M. and Oberhauser, A.F. The Effects of Pathogenic Mutations on the Nano-mechanics of PKD Domains. The 5th Annual Research Retreat 2008. University of Texas Medical Branch, Galveston, TX, July, 2008
- ***Ma, L.***, Xu, M. and Oberhauser, A.F. The Effects of Pathogenic Mutations on Polycystin-1 Mechanical Properties. The 13th Annual Structural Biology Symposium 2008. UTMB,

Galveston, TX, May, 2008

- ***Ma, L.***, Xu, M. and Oberhauser, A.F. The Effects of Pathogenic Mutations on Polycystin-1 Mechanical Properties. The Joint Meeting of the Biophysical Society 52nd Annual Meeting & 16th International Biophysics Congress. Long Beach, CA, February, 2008
- ***Ma, L.***, Xu, M. and Oberhauser, A.F. The Effects of Pathogenic Mutations on Polycystin-1 Mechanical Properties. The 47th Annual Meeting of the American Society for Cell Biology. Washington, DC, December, 2007
- ***Ma, L.***, Garcia, T. and Oberhauser, A.F. The Nanomechanics of Polycystin-1. "Molecules and Mechanisms" 4th Annual Research Retreat 2007. University of Texas Medical Branch, Galveston, TX, November, 2007
- ***Ma, L.***, Garcia, T. and Oberhauser, A.F. The Nanomechanics of the REJ Region of Polycystin-1. The 12th Annual Structural Biology Symposium 2007. University of Texas Medical Branch, Galveston, TX, May, 2007
- ***Ma, L.***, Garcia, T. and Oberhauser, A.F. The Nanomechanics of Polycystin-1. "Molecules and Mechanisms" 4th Annual Research Retreat 2007. University of Texas Medical Branch, Galveston, TX, May, 2007
- ***Ma, L.*** Genetic studies for stock enhancement of red drum (*Sciaenops ocellatus*) in Texas bays and estuaries. Texas Bays and Estuaries Meeting 2005. Port Aransas, TX, April, 2005